



MARMARA UNIVERSITY
FACULTY OF ENGINEERING



**ANALYSIS OF STRESSES OCCURRING IN THE
STATIC AND DYNAMIC STATES OF HIGH-
CAPACITY FEEDERS USED IN THE MINING AND
AGGREGATE INDUSTRY AND DESIGN
IMPROVEMENTS**

VEDAT NEDİM DOĞAN
MERYEM ÇAPAR

GRADUATION PROJECT REPORT
Department of Mechanical Engineering

Supervisor
Prof. Dr. Paşa YAYLA

ISTANBUL, 2023



MARMARA UNIVERSITY
FACULTY OF ENGINEERING



Analysis of Stresses Occurring in the Static and Dynamic States of High-Capacity Feeders Used in the Mining and Aggregate Industry and Design Improvements

by

**Vedat Nedim DOĞAN
Meryem ÇAPAR**

June 08, 2023, Istanbul

**SUBMITTED TO THE DEPARTMENT OF MECHANICAL ENGINEERING IN
PARTIAL FULFILLMENT OF THE REQUIREMENTS FOR THE DEGREE
OF
BACHELOR OF SCIENCE
AT
MARMARA UNIVERSITY**

The authors hereby grant to Marmara University permission to reproduce and to distribute publicly paper and electronic copies of this document in whole or in part and declare that the prepared document does not in any way include copying of previous work on the subject or the use of ideas, concepts, words, or structures regarding the subject without appropriate acknowledgement of the source material.

Signature of Author(s) **Vedat Nedim DOĞAN**.....

Meryem ÇAPAR.....

Department of Mechanical Engineering

Certified by **Prof.Dr. Paşa YAYLA**.....

Project Supervisor, Department of Mechanical Engineering

Accepted by **Prof.Dr. Bülent EKİCİ**.....
Head of the Department of Mechanical Engineering

TABLE OF CONTENTS

ACKNOWLEDGEMENTS	iv
ÖZET	v
ABSTRACT	vi
SYMBOLS	vii
ABBREVIATIONS	viii
LIST OF FIGURES	ix
LIST OF TABLES	xi
1. INTRODUCTION	1
1.1 Background.....	1
1.2 Problem Statement	1
1.3 Literature Review.....	2
1.3.1 Vibratory Feeders.....	2
1.3.2 Modal Analysis and FEA Method.....	4
1.3.3 Finite Element Model of Vibrating Feeders.....	5
1.3.4 Modal Analysis of Vibrating Feeders	5
1.3.5 Mathematical Background	5
1.3.6 Fatigue of Feeder	7
1.4 Scope of Research.....	8
2. PRACTICAL INVESTIGATION.....	9
2.1 CAE Software	9
2.2 Selecting ANSYS.....	10
2.3 Geometry Cleaning	11
3. ANALYSIS.....	12
3.1 Stress Analysis	16
3.1.1 Preparations for Stress Analysis	16
3.1.2 Results of Stress Analysis	24
3.2 Vibration Analysis	29
3.2.1 Preparation for Vibration Analysis	29
3.2.2 Results of Vibration Analysis	31

3.3 Fatigue Analysis	37
3.3.1 Preparation for Fatigue Analysis.....	37
3.3.2 Results of Fatigue Analysis.....	38
3.4 Analysis of Critical Frequencies	43
3.4.1 Total Deformations for First Feeder at Critical Frequencies.....	43
3.4.2 Total Deformations of Second Feeder at Critical Frequencies	46
3.5 Effect of Meshing Process on Analysis	49
4. CONCLUSION AND DISCUSSION.....	53
4.1 Conclusion of Thesis.....	53
4.2 Recommendations for Future Works	55
4.3 Evaluation of Current Work from MUDEK Perspective	56
4.3.1 Economic Analysis	56
4.3.2 Real-Life Conditions.....	56
4.3.3 Producibility.....	56
4.3.4 Constraints	56
REFERENCES	57
APPENDICES	60
.....	61

ACKNOWLEDGEMENTS

We would like to acknowledge and give our warmest thanks to my supervisor, Prof. Dr. Paşa YAYLA, who made this work possible. His guidance and advice carried us through all the stages of writing our thesis. His insight and direction have made us better engineers by improving both our critical thinking skills and the methods we use to analyze complex engineering problems. We would also like to thank our committee members for letting us defend and for your thoughtful comments and suggestions.

We would like to thank Özge GÜLER, Research and Development Manager of Burçelik A.Ş., for showing us her continuous support and cooperation.

We would also like to thank Ceren GENÇ and Mert ATAK, who helped us to analyze the process.

We also would like to thank TÜBİTAK for supporting our project within the scope of the 2209-B University Students Industrial Research Projects Support Program, which provides financial resources and materials for us.

ÖZET

Titreşimli besleyiciler, malzemelerin transferini kolaylaştırarak birçok endüstride hayatı bir rol oynamaktadır. İdeal malzeme akış hızına ulaşmak, besleyicinin verimli çalışmasına bağlıdır. Bu makale, statik ve dinamik aşamalar sırasında yaşanan stres değişimlerini ayırt etmeyi amaçlayan deneysel bir araştırmayı ele almaktadır. Titreşimli besleyici, ANSYS kullanılarak incelenmiştir.

Titreşimli besleyiciler, birçok endüstride malzeme taşıma uygulamalarında yaygındır. Bu araştırma makalesi, belirli bir titreşimli besleyici tipinin stres ve deformasyon problemini incelemektedir. Ayrıca titreşimli besleyici teknolojisinin arkasındaki teoriyi ve tasarımının önemini açıklığa kavuşturur.

Sonlu elemanlar yöntemi, bu yorgunlukları tespit ederek ve yorulma bölgelerini analiz ederek olası bir kırılmayı önler ve bize fikir verir.

ABSTRACT

Vibratory feeders play a vital role in numerous industries by facilitating the transfer of materials. Achieving the ideal material flow rate depends on the feeder's efficient functioning. This thesis delves into an experimental inquiry that aims to discern the variations in stress experienced during the static and dynamic phases. The vibrating feeder was studied using ANSYS.

Vibrating feeders are standard in material handling applications across multiple industries. This thesis examines the stress and deformation problems of a particular vibrating feeder type. It also clarifies the theory behind vibratory feeder technology and the importance of its design.

By detecting these fatigues and analyzing the fatigue zones, the finite element method prevents possible breakage and gives us an idea.

SYMBOLS

<u>Symbol</u>	<u>Name</u>	<u>Unit</u>
A	Area	m^2
c	Damping coefficient	$\text{kg}\cdot\text{m}^{-1}\cdot\text{s}^{-1}$
c_{eq}	Equivalent damping coefficient	$\text{kg}\cdot\text{m}^{-1}\cdot\text{s}^{-1}$
F	Force	$\text{kg}\cdot\text{m}\cdot\text{s}^{-2}$
$f(t)$	Force as a function of time	$\text{kg}\cdot\text{m}\cdot\text{s}^{-2}$
G	Shear modulus	$\text{kg}\cdot\text{m}^{-1}\cdot\text{s}^{-2}$
k	Stiffness coefficient	$\text{kg}\cdot\text{s}^{-2}$
l	Stretched spring length	m
l_0	Unstretched spring length	m
Δl	Change in length	m
m	Mass	Kg
x	Displacement	m
γ	Shear strain	
$\Delta\gamma$	Change in shear strain	
E	Young's modulus	$\text{kg}\cdot\text{m}^{-1}\cdot\text{s}^{-2}$
ϵ	Strain	
$\Delta\epsilon$	Change in strain	
σ	Stress	$\text{kg}\cdot\text{m}^{-1}\cdot\text{s}^{-2}$
$\Delta\sigma$	Change in stress	$\text{kg}\cdot\text{m}^{-1}\cdot\text{s}^{-2}$
r	Shear stress	$\text{kg}\cdot\text{m}^{-1}\cdot\text{s}^{-2}$
Δr	Change in shear stress	$\text{kg}\cdot\text{m}^{-1}\cdot\text{s}^{-2}$
ω_F	Operating frequency	$\text{rad}\cdot\text{s}^{-1}$

ABBREVIATIONS

FEA	: Finite Element Analysis
FEM	: Finite Element Method
SQP	: Sequential Quadratic Programming
SDOF	: Single Degree of Freedom

LIST OF FIGURES

Figure 1.1 Optimization process.....	3
Figure 1.2 System dynamics of vibrating feeder	6
Figure 1.3 Vibratory feeder	7
Figure 2.1 CAE software's tree	10
Figure 2.2 ANSYS working principle	10
Figure 3.1 How to open SpaceClaim on ANSYS Workbench	12
Figure 3.2 Isometric view of first feeder	12
Figure 3.3 Top view of first feeder.....	13
Figure 3.4 Left view of first feeder.....	13
Figure 3.5 Bottom view of first feeder	14
Figure 3.6 Isometric view of second feeder.....	14
Figure 3.7 Top view of second feeder	15
Figure 3.8 Right view of second feeder.....	15
Figure 3.9 Bottom view of second feeder.....	16
Figure 3.10 A part example of made angular by deleting the radius	17
Figure 3.11 Holes on the right plate of the feeder	17
Figure 3.12 Cylinders to be used as springs	17
Figure 3.13 Point masses used instead of engines	18
Figure 3.14 Created new coordinate systems	19
Figure 3.15 Engineering data tab.....	19
Figure 3.16 Example of contact controlling	20
Figure 3.17 Details about one of the contact	20
Figure 3.18 Details and options of mesh operation for the first feeder	21
Figure 3.19 First feeder's isometric view after mesh operation	21
Figure 3.20 Details and options for the second feeder	21
Figure 3.21 Isometric view of the second feeder after mesh operation	22
Figure 3.22 Forces of 1000 N applied to plate	22
Figure 3.23 Forces of 71,43 N applied to the grids	23
Figure 3.24 Fixed supports	23
Figure 3.25 Stress analysis - total deformation for the first feeder.....	24
Figure 3.26 Stress analysis - equivalent elastic strain for the first feeder.....	25
Figure 3.27 Stress analysis - equivalent (von-Mises) stress for the first feeder	26
Figure 3.28 Stress analysis - total deformation for the second feeder	27
Figure 3.29 Stress analysis - equivalent elastic strain for the second feeder	28
Figure 3.30 Stress analysis - equivalent (von-Mises) stress for the second feeder.....	29
Figure 3.31 Connecting static structural's model to modal's model.....	30
Figure 3.32 Analysis setting tab	30
Figure 3.33 Connecting modal's solution to response spectrum's setup	30
Figure 3.34 Frequency data of the engine	31
Figure 3.35 Vibration Analysis - Equivalent Stress critical areas for the first feeder	31

Figure 3.36 Vibration Analysis - Equivalent Stress for the first feeder.....	32
Figure 3.37 Vibration Analysis - Total Deformation at 50,169 Hz for the first feeder	32
Figure 3.38 Vibration Analysis - Total Deformation for first feeder.....	33
Figure 3.39 Vibration Analysis - Normal Elastic Strain on X Axis for first feeder	34
Figure 3.40 Vibration Analysis - Equivalent Stress Red Areas for the second feeder	34
Figure 3.41 Vibration Analysis - Equivalent Stress for the second feeder	35
Figure 3.42 Vibration Analysis - Total Deformation for second feeder	35
Figure 3.43 Vibration Analysis - Total Deformation at 50,462 Hz for second feeder	36
Figure 3.44 Vibration Analysis - Normal Elastic Strain on X Axis for second feeder.....	36
Figure 3.45 Connecting response spectrum's model to static structural's model	37
Figure 3.46 Fatigue Tool	37
Figure 3.47 Static preparations for fatigue analysis	38
Figure 3.48 Grouping of forces	38
Figure 3.49 Fatigue Analysis - Life for the first feeder	39
Figure 3.50 Fatigue Analysis - Life critical point for the first feeder	39
Figure 3.51 Fatigue Analysis - Damage for first feeder	40
Figure 3.52 Fatigue Analysis - Damage red area for the first feeder	40
Figure 3.53 Fatigue Analysis - Safety Factor for the first feeder	41
Figure 3.54 Fatigue Analysis - Life for second feeder	41
Figure 3.55 Fatigue Analysis - Damage for second feeder.....	42
Figure 3.56 Fatigue Analysis - Safety Factor for second feeder.....	42
Figure 3.57 Total deformation of first feeder at 10,773 Hz.....	43
Figure 3.58 Total deformation of first feeder at 16,336 Hz.....	43
Figure 3.59 Total deformation of first feeder at 26,176 Hz.....	44
Figure 3.60 Total deformation of first feeder at 33,076 Hz.....	44
Figure 3.61 Total deformation of first feeder at 41,475 Hz.....	45
Figure 3.62 Total deformation of first feeder at 50,89 Hz.....	45
Figure 3.63 Total deformation of second feeder at 10,594 Hz	46
Figure 3.64 Total deformation of second feeder at 15,729 Hz	46
Figure 3.65 Total deformation of second feeder at 26,54 Hz	47
Figure 3.66 Total deformation of second feeder at 34,477 Hz	47
Figure 3.67 Total deformation of second feeder at 43,101 Hz	48
Figure 3.68 Total deformation of second feeder at 50,271 Hz	48
Figure 3.69 First meshing details of first feeder	49
Figure 3.70 First feeder's isometric view after first meshing	49
Figure 3.71 First meshing details of second feeder	50
Figure 3.72 Second feeder's isometric view after first meshing	50
Table 3.2 Stress results from first and second meshings for first and second feeders	51
Table 3.3 Total deformation results from first and second meshings for first and second feeders.....	51
Table 3.4 Fatigue analysis results from first and second meshings for first and second feeders.....	52

LIST OF TABLES

Table 3.1 Document from the company showing the weight of the engine	18
Table 3.2 Stress results from first and second meshings for first and second feeders	51
Table 3.3 Total deformation results from first and second meshings for first and second feeders.....	51
Table 3.4 Fatigue analysis results from first and second meshings for first and second feeders.....	52

1. INTRODUCTION

This study consists of four main parts focusing on information about vibratory feeders. This study compares various literature studies, allowing the subject to be explored in detail. The first part focuses on the purpose of the research while providing information on the feeders' modelling, optimization and operation. The first part leads the work by laying the foundation for the subsequent chapters. In addition, the first part explains the impact of the FEM method on research and the potential and limitations of simulation's contribution to error detection. The second part gives information about the feeder analysis and previous analysis studies that were made by leading the third part. The last part of the study collects all the results, compares the analysis results and talks about the economic and manufacturability benefits of the study.

1.1 Background

The vibrating feeder plays a vital role in material processing in industrial and mining enterprises. Comprising key components such as a vibratory drive unit, vibratory feeder bowl, amplitude controller and inline feeder and track, it uses vibration to "feed" material to a process or machine. However, excessive vibration can lead to the failure of vibratory feeders, affecting their performance and reliability.

1.2 Problem Statement

Recently, there has been a significant focus on optimizing both the efficiency and the geometry of vibratory feeders. This increased attention highlights the unique interest and dedication towards enhancing performance.

However, despite the extensive efforts in optimizing vibratory feeders, there needs to be more research dedicated to exploring the potential of utilizing a model of a feeder to provide insights into its performance and aid in the identification of failures or damages. This gap in research creates a unique opportunity for further exploration and investigation.

1.3 Literature Review

The literature review is divided into five main sub-topics focusing on different branches related to vibratory feeders. This section provides a comprehensive understanding of the subject and compares different and existing literature.

The first topic delves into the subject, covering various aspects such as design, operating principles and optimization of feeders. It also introduces the FEM method and its use in feeders, which will be discussed in detail later in the thesis. This chapter provides a solid foundation for the next chapters by describing the method and its operation.

The second research area generally explains the importance of the Finite Element Method (FEM) model in the thesis and talks about modal analysis.

The next sections of the literature review examine the methods in detail. This review was based not only on individual research but also on the available knowledge in the field.

1.3.1 Vibratory Feeders

This chapter delves into the topic of vibratory feeders, taking a closer look at the key components required for research and development. Topics covered include error detection, modeling techniques, and the optimization process for vibrating feeders.

The dominant methodology used in the design of vibrating screens first involves modelling the feeder using Finite Element Method (FEM) software. By running the feeder modelling in a FEM environment, it becomes possible to change parameters without requiring a new feeder to be produced for each design iteration. Building a FEM model represents an economical and simple substitute for setting parameters in a real feeder. The procedure for developing a FEM model for the feeder finds application both in increasing material handling efficiency and in simulating faults in vibrating feeders. Currently, the following types of FEA analysis are used: static analysis, modal analysis, harmonic analysis, temporal dynamic analysis, spectrum analysis, buckling analysis, and open dynamic analysis (Ramatsetse et al., 2017).

A comprehensive investigation was conducted using ANSYS, a cutting-edge software for

engineering analysis, encompassing modal analysis and harmonic response analysis. These meticulous analyses yielded a wealth of dynamic data. Among the invaluable insights gained was determining natural frequencies, intricate mode shapes, and stress and strain distribution throughout the structure. This groundbreaking research has paved the way for an unprecedented understanding of the vibrating feeder's behaviour.

Optimization is a mathematical technique that aims to find the lowest or highest values of specified functions while considering a set of limitations or conditions. When it comes to design, optimizing machine components is an important process that leads to creating high-quality products while minimizing costs. This approach is frequently employed to enhance vibrating feeder designs, optimize frequency (Csizmadia et al., 2011), and improve productivity (Wang et al., 2012), ultimately ensuring seamless and efficient operation.

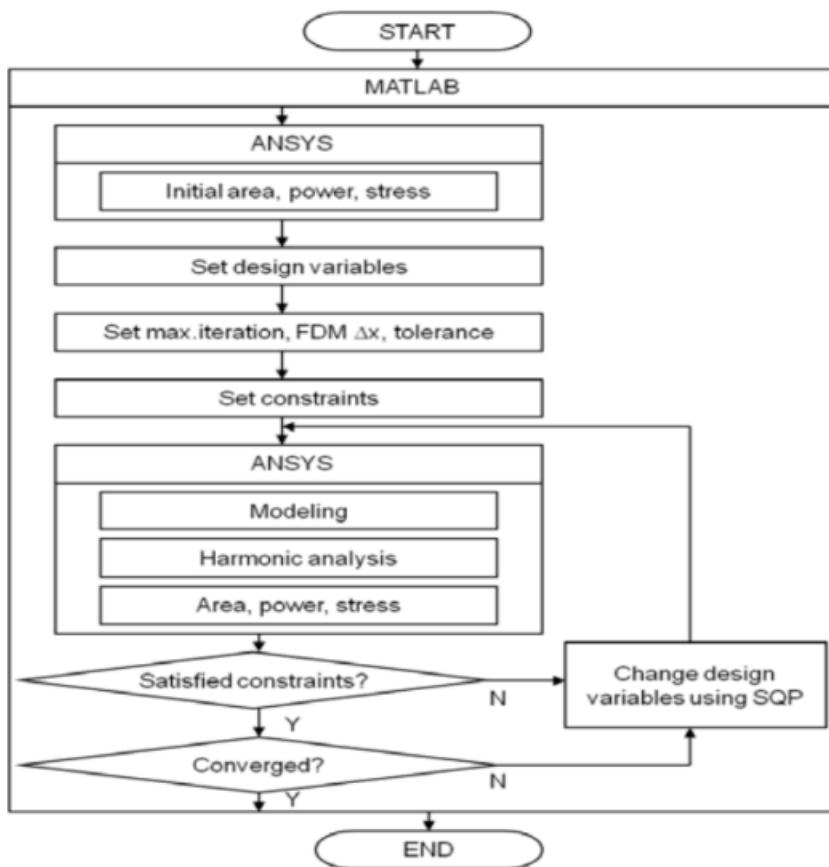


Figure 1.1 Optimization process

Optimizing vibratory feeders is straightforward: enhancing profitability ('Vibration analysis of vibrating screens', 2012). Various methods are employed to increase the efficiency of vibratory feeders, such as reducing energy consumption, improving

productivity, minimizing downtime, and streamlining maintenance. In the study conducted by Yue-Min et al. (2009), the reliability of vibrating screens is enhanced by optimizing the size of the stiffeners on the side plate, taking into account multiple frequency constraints. This optimization reduced the weight of the side plates and resulted in an increase in natural frequencies, effectively moving them away from the operating frequency. Production costs have decreased as the weight of the screen has decreased. Also, moving the natural frequency away from the operating frequency improved resonance avoidance, reducing potential damage to the screen. By reducing the screen's weight, manufacturing costs were reduced. Moreover, relocating the natural frequency away from the operating frequency improved the avoidance of resonance, thereby mitigating potential damage to the screen.

1.3.2 Modal Analysis and FEA Method

Modal analysis through FEM (Finite Element Method) has emerged as an invaluable tool for evaluating structural elements, primarily due to its reliability and cost-effectiveness. This analysis technique provides a comprehensive understanding of structural behavior by operating within a virtual environment offered by software platforms (Ramsey, 1983).

The modal analysis uncovers essential insights by determining dynamic structures' natural frequencies and mode shapes (Raoa, 2012). To capture the structure's dynamic characteristics, a concise selection of initial mode shapes, accompanied by their corresponding natural frequencies, suffices (Carr, 1994). Symmetrical structures exhibit multiple modes in different directions, characterized by similar natural frequencies (Carr, 1994). Applying structural modal analysis extends to detecting failures within the structure and its components, enabling comprehensive assessment and troubleshooting (Rytter, 1995).

Within the context of vibratory feeders, the FEM method finds utility in harmonic response analysis. The harmonic analysis identifies a structure's steady-state response, allowing for the mitigation of resonance and fatigue induced by forced vibrations (Shelot, 2014). This crucial analysis aids in optimizing the design and performance of vibratory feeders, ensuring their efficient and reliable operation in various industrial applications.

1.3.3 Finite Element Model of Vibrating Feeders

To optimize operational efficiency and reduce cell count, a simplification approach based on the three-dimensional model can be employed. Recognizing the inherent symmetry of the vibrating feeder's structure and the corresponding force and installation forms, an analysis utilizing only half of the model becomes feasible. Additionally, standard connectors such as bolts can be eliminated, and welding assemblies can be treated as cohesive entities by removing individual welds. Details such as bolt holes and fillets that have minimal impact on the analysis can be disregarded. In contrast, non-essential components such as the discharge port, feed inlet, and supporting device can be excluded from consideration. Instead, a spring-like "connector" can be defined to simulate their influence.

This simplified technique allows for a more efficient and targeted study of the vibrating feeder. The simplified model minimizes computational complexity and allows engineers to focus on the important parts of the feeder's behavior, resulting in greater understanding and practical outcomes.

1.3.4 Modal Analysis of Vibrating Feeders

The modal analysis is an important method for optimizing the performance of vibrating feeders. By accurately establishing the feeder's natural frequencies and forms, useful insights are gleaned that may be used to improve the design and enable dynamic response analysis. The rigorous elimination of extraneous factors before analysis provides a concentrated assessment of inherent traits. The modal analysis allows for greater performance, dependability, and operational efficiency.

1.3.5 Mathematical Background

The vibratory feeder mathematical model is essential in its ability to reflect the behavior and dynamics of the system. The model captures the main features of the vibrating feeder and provides a mathematical understanding of its operation, taking into account forced vibration in the Single Degree of Freedom (SDOF) system. Including key components such as the chute, support structure, coil springs, and engine arrangement enhances the model's authenticity. These components are essential for the feeder to work and play critical roles in defining its behavior. It is also distinctive that the model uses a sinusoidal

external force to generate vibration. This type of excitation is often used in vibratory feeders and successfully produces the required feeding effects. This mathematical model is important due to the vibrating feeder system's complete modeling, including critical components, an inclined trough, and sinusoidal excitation. Considering these factors, the model provides a valuable tool for analyzing and optimizing the performance of vibratory feeders in various applications.

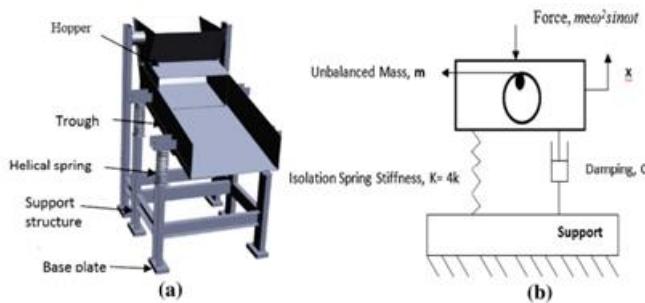


Figure 1.2 System dynamics of vibrating feeder (Chandravanshi, 2015)

The exciting sinusoidal force can be represented as $F_0 \sin \omega t$, where F_0 is the magnitude of the external excitation force. The equation describing the force vibration can be expressed as follows.

$$M \frac{d^2x}{dt^2} + c \frac{dx}{dt} + Kx = F_0 \sin \omega t$$

Here, M represents the mass of the trough, which includes the vibratory motor. Including the vibratory motor in the mass calculation distinguishes this model, as it accounts for the additional weight and dynamics the motor introduced.

K denotes the combined stiffness of the four helical springs on which the trough is installed. The use of helical springs as the supporting mechanism adds uniqueness to the model, as it affects the overall stiffness and response of the system.

C represents the damping characteristics of the system. The consideration of damping is essential for an accurate representation of the vibratory feeder's behavior. It accounts for the energy dissipation and influences the overall vibration dynamics.

By incorporating these parameters - the mass of the trough including the vibratory motor,

the combined stiffness of the helical springs, and the damping characteristics of the system - the model captures the specific attributes of the vibratory feeder under analysis, making it unique in its representation and characterization of the system's dynamics.

The springs are first modeled with a fully elastic behavior (Childs, 2004), with the longitudinal and transversal stiffness determined by:

$$D_E \nabla^4 w(x, y, t) + [\rho + m_c \delta(x - u) \delta(y - v)] \frac{\partial^2 w}{\partial t^2} = 0$$

where $D_E = E_Y/(12(1-v^2))$ is the bending stiffness. (Singh,2022)

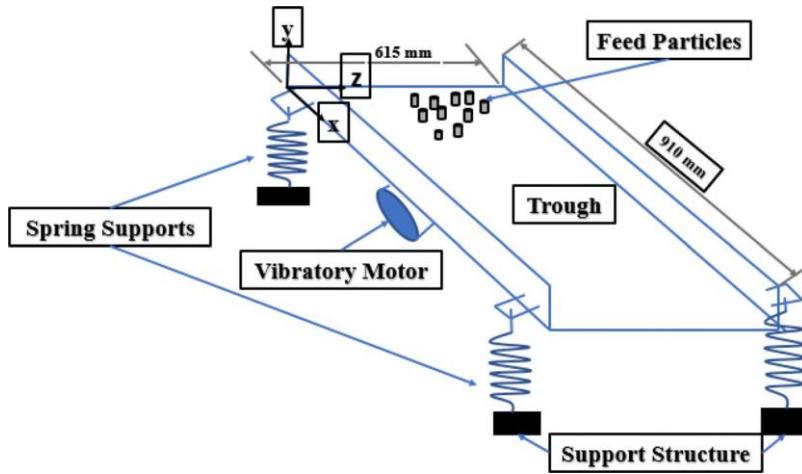


Figure 1.3 Vibratory feeder (Singh,2022)

1.3.6 Fatigue of Feeder

Fatigue is thought to be responsible for up to 90% of all design-related failures (Pope, 1997, p. 330). Fatigue failures are typically caused by the fact that most design issues are overcome during the early phases of a product's development. However, fatigue issues do not show until the product has been subjected to several cycles. It is quite likely that the product is already in service at this point in its lifespan. Fatigue cracking occurs most commonly in metallurgical flaws like voids or inclusions, as well as design elements like fillets, screw threads, or bolt holes. Cracking can begin in any severely pressured area. It is also worth noting that cracking can occur during manufacture but may only appear after a lengthy period of use (Pope, 1997). Many components are subject to constantly changing stresses/strains, and the resulting fatigue plays a role in all situations (Coffin, 1979).

1.4 Scope of Research

In this seminal article, we embark on a comprehensive study centered around a knockout machine as the primary object of scrutiny. We aim to conduct a meticulous investigation, analyzing stress distribution and deformation under both static and dynamic loads on vibratory feeder. Notably, the vibrating feeder experiences forceful vibrations under high-intensity loads, making it prone to fatigue failure. Due to the intricate nature of its complex structure and shape, traditional design methods must be revised to accurately assess the resulting stress levels.

2. PRACTICAL INVESTIGATION

Dynamic studies of the feeder were performed to gather information about strength and deformities under force. These measurements were made for various reasons. Preventing and testing for breakage before it happens. Determining the maximum force, it can carry and Its effect on velocity and acceleration.

The robustness of vibratory equipment structures is paramount as they undergo significant dynamic forces, and preliminary design can lead to premature failures. Metal fatigue, resulting from continuous dynamic loading and eventually leading to cracking and complete failure under high stresses, necessitates a thorough understanding of the vibratory system and the loads it transfers to its supporting structure. Specifically, in the case of a vibratory feeder, the forces exerted pose a significant challenge, demanding an exceptionally sturdy support structure capable of withstanding dynamic loads that surpass the static load (McMilan, 2011).

This part of the thesis is divided into two sub-titles. The first part explains the selection of the preferred program for fatigue and cracking and stress analysis and its reasons. In the second part, the importance of the preliminary preparations made at the beginning of the analysis in this program and what has been done in general are mentioned.

2.1 CAE Software

CAE stands for Computer Aided Engineering. It is basically the use of computers to solve engineering issues before creating and testing a physical prototype. CAE analyzes, validates, and optimizes a product's or structure's performance in diverse operating situations. It will utilize the CAD data or model as the input for this purpose. We must consider some criteria when choosing a program to analyze the CAE software varieties. When considering factors such as the number of elements or nodes it can handle, maximum model size, and any limitations on the geometry or meshing capabilities, ANSYS is the best choice among them.

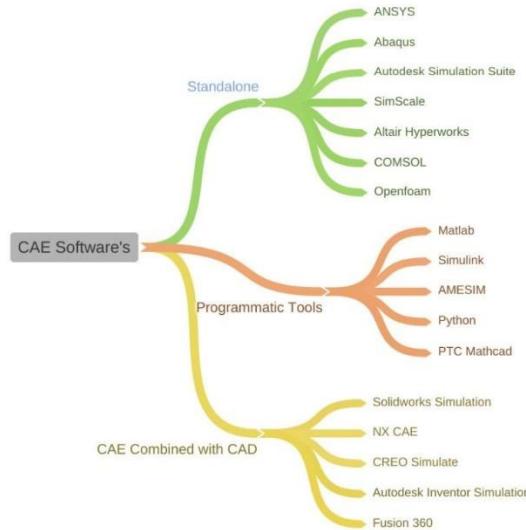


Figure 2.1 CAE software's tree(McMillan,2011)

2.2 Selecting ANSYS

ANSYS is a mechanical product design and civil structure design analysis program. It solves issues using computer-based numerical approaches. It is ANSYS Inc.'s FEA software. It is commonly used in the business for analyzing solutions. It can address a wide variety of problems. It aids in the engineering and construction of sophisticated, highly nonlinear, big models. It is used to excite computer models of buildings, electronics, or machine components for strength, elasticity, and temperature analysis. The ANSYS Workbench system is used for the majority of its stimulation. It also creates data management and backup software.

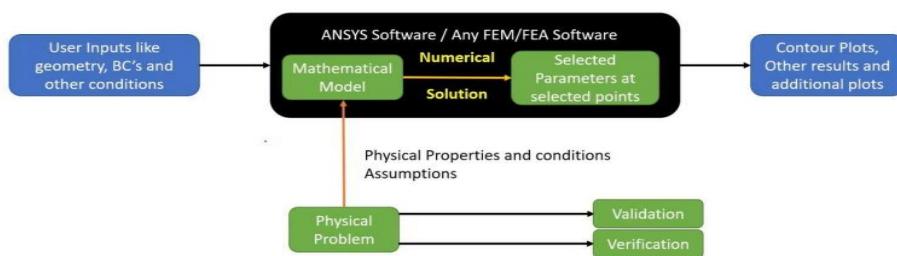


Figure 2.2 ANSYS working principle (McMilan,2011)

The most important reasons for using ANSYS in this model are that ANSYS performs advanced simulations correctly, optimizes various features such as geometry boundary conditions, and can import and run the model from different CAD software.

Also, ANSYS provides sophisticated meshing tools that enable users to create high-quality meshes for accurate simulations. It includes structured, unstructured, and hybrid meshing techniques, as well as features like automated mesh adaption for enhanced accuracy and efficiency. This allows us to manually select the mesh suitable for the parts, increasing the reliability of the solution.

2.3 Geometry Cleaning

When utilizing ANSYS or any other CAE program, geometry cleaning and import are critical phases in the analysis process. Clean and correct geometry guarantees dependable and valid analytical findings, while good import ensures that the model is accurately represented. These processes improve computational performance, permit correct boundary condition application, simplify simulation setup, and improve result interpretation. Because of the existence of dirty geometry when geometry is not cleaned prior to analysis, producing a mesh becomes problematic. Mesh algorithms rely on well-defined and linked surfaces, edges, and vertices. Unclean geometry can result in poorly shaped pieces, a mix of multiple element types, or even full mesh generation failure. As a result, this might lead to decreased accuracy, difficulties obtaining convergence, or greater processing needs during analysis. Finding computers capable of managing the resulting complicated and time-consuming mesh is also difficult.

In the analysis section, geometry cleaning and other analysis preparations made before each analysis in the model is included.

3. ANALYSIS

Two feeder designs were sent, modelled and produced by BURCELİK company via CAD software. The reason for having two is that after the first feeder was produced and sent to the company's customer, there were some problems, and the second design was made with minor updates with feedback from the customer. The problems were solved in the second design. The main goal is to make detailed static and dynamic analyses through two feeders ANSYS.

The two feeder designs were sent as files with .stp extension. First, these .stp files were opened with the help of the SpaceClaim service of ANSYS.

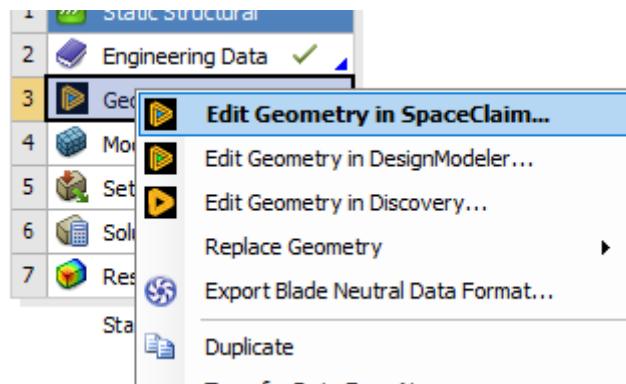


Figure 3.1 How to open SpaceClaim on ANSYS Workbench

First, the first feeder design was unveiled on the SpaceClaim service.

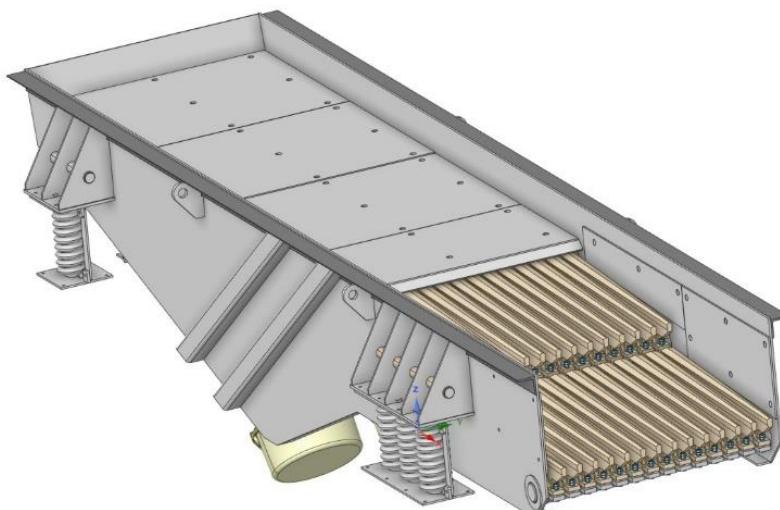


Figure 3.2 Isometric view of first feeder

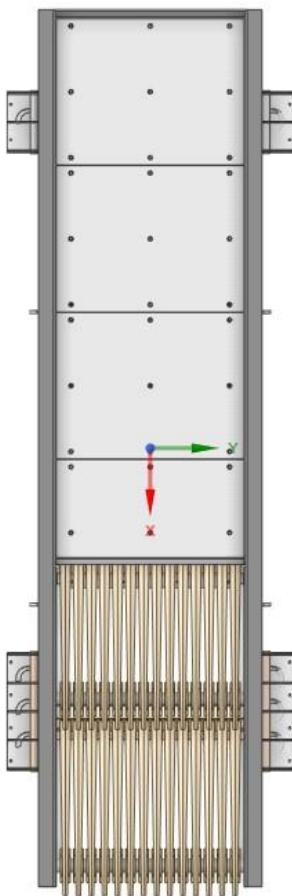


Figure 3.3 Top view of first feeder

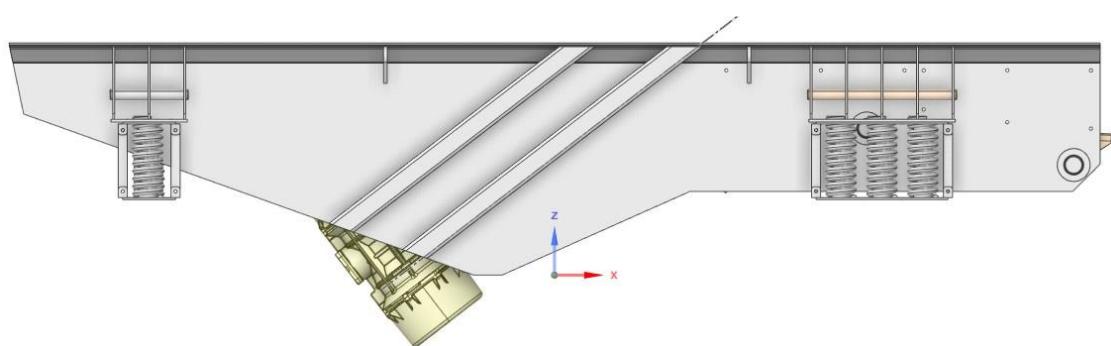


Figure 3.4 Left view of first feeder

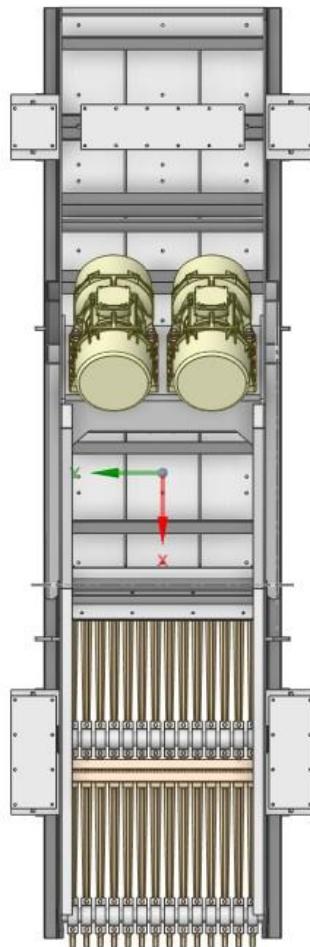


Figure 3.5 Bottom view of first feeder

Then the second feeder design was unveiled at SpaceClaim service.

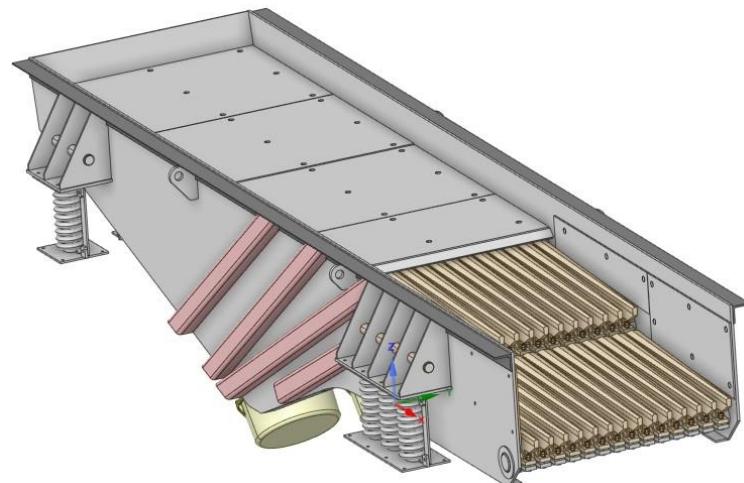


Figure 3.6 Isometric view of second feeder

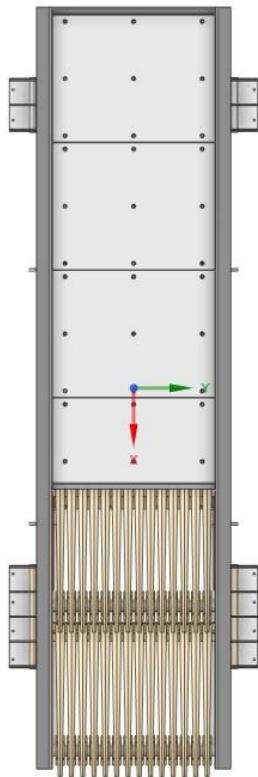


Figure 3.7 Top view of second feeder

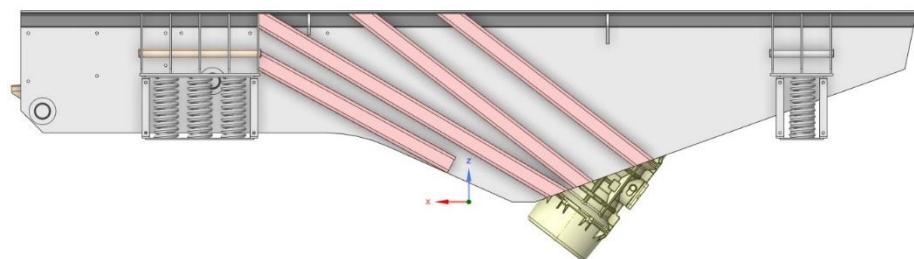


Figure 3.8 Right view of second feeder

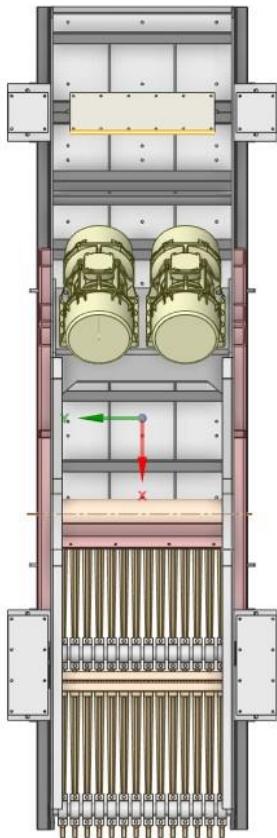


Figure 3.9 Bottom view of second feeder

3.1 Stress Analysis

3.1.1 Preparations for Stress Analysis

Some preparations had to be made to perform stress analyses of both feeder designs correctly. The preparations for both feeders are the same. It would be convenient to compare them while having the same boundary conditions.

In order to perform the mesh operation correctly and without errors, first of all, a process called geometry cleaning was performed. In this process called geometry cleaning, minimizing the factors that may affect the meshing process is essential. The first step of the geometry cleaning was to delete all the radius areas in the design and turn them into corners.

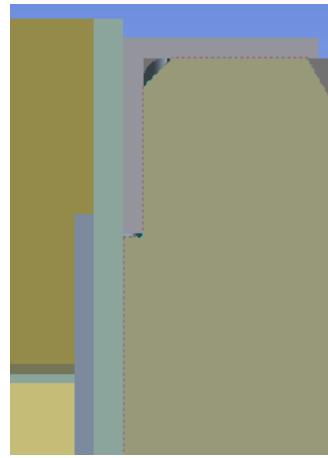


Figure 3.10 A part example of made angular by deleting the radius

After all the radii were turned into corners, or other process, the circle arrangement, was done. This step is to fill the holes opened at an angle to place the screws, one by one, by filling only in a circle.

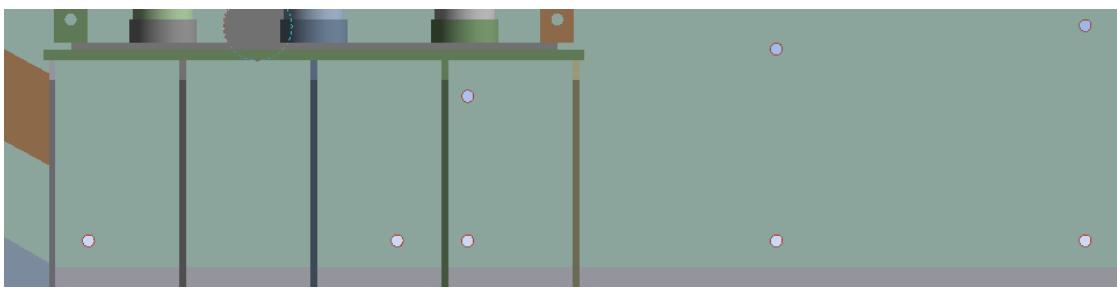


Figure 3.11 Holes on the right plate of the feeder

After the recesses were also arranged, the springs were simplified. The complex structure of the springs is one of the factors affecting the meshing process. Therefore, the springs were deleted and replaced by cylinders of the same diameter and length to act as springs.

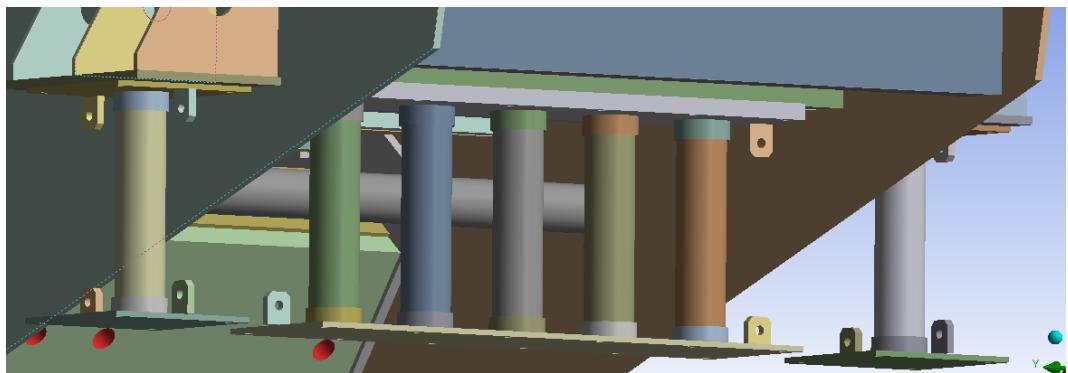


Figure 3.12 Cylinders to be used as springs

Like the springs, the large motors of these feeders are also factors that can affect the meshing process. Therefore, the engines were deleted and replaced by 2-point masses equal to the number of engines.

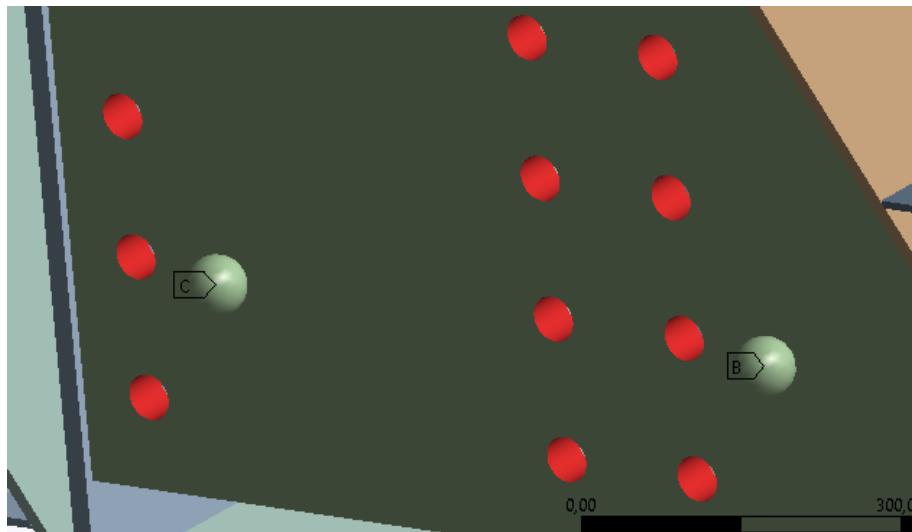


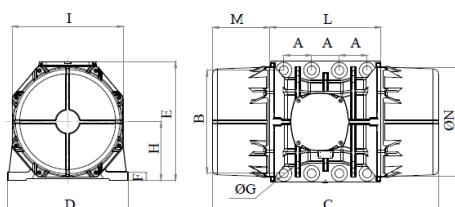
Figure 3.13 Point masses used instead of engines

A weight had to be specified for each point mass in point masses. These weights had to be equal to the weights of the engines. These weights were set as 768 kg from the technical report received by the company.



MVE 19500/1E-105A0 [EE619500A5A08A0000]
3 PH - 6 kutup - 1000 d/d - 380-415 V [Delta] - 50 Hz

Çalışma momenti (Kg*cm)	Vibratör çekicileri (Kg*cm)	Santrifij kuvveti (Kg)	Nominal voltaj [V]	Giriş gücü (kW)	Akım [A]	Güç faktörü	Ia/In
3.632	1.816	20.285	380-415 [Delta]	11,96	△ 24	0,72	5,4



Ağırlık [Kg]	TÜM EBATLAR [mm]												
	A	B	G	Delik sayısı	C	D	E	F	H	I	L	M	N
768	140	480	45	8	1.060	570	542	48	268	510	560	250	490

Table 3.1 Document from the company showing the weight of the engine

Action had to be taken to correctly attach and place the point masses. This process was to assign a new coordinate system to the origin of the point masses.

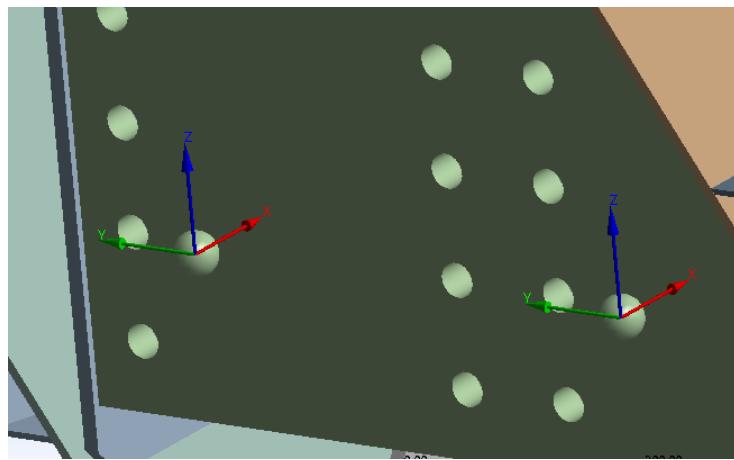


Figure 3.14 Created new coordinate systems

After the new coordinate system was determined, materials with their own properties were selected for the correct evaluation of springs and motors in the analysis. Unless you add it in the ANSYS Mechanical service, the whole body appears to be made of a single material, automatically called structural steel. In ANSYS Workbench, materials with properties for both spring and motor were entered from the Engineering Data section.

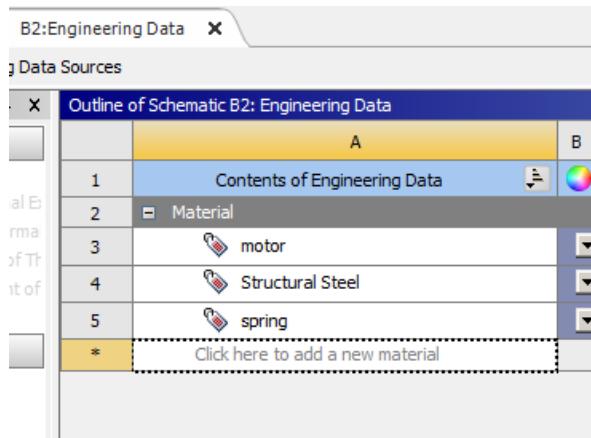


Figure 3.15 Engineering data tab

In ANSYS Mechanical, in the Geometry tab, the point masses and cylinders added instead of springs and motors have been assigned their own materials separately from the properties tab.

After this process, there was the control of the contacts, which was the last operation to be done for the correctness of the Mesh operation. All contacts were made and checked one

by one with the Contact Tool option in the Connections tab. If this is not done, ANSYS detects the parts separately and gives analysis results as if they are independent from each other. 726 contacts for the first feeder and 768 contacts for the second feeder were defined and controlled.

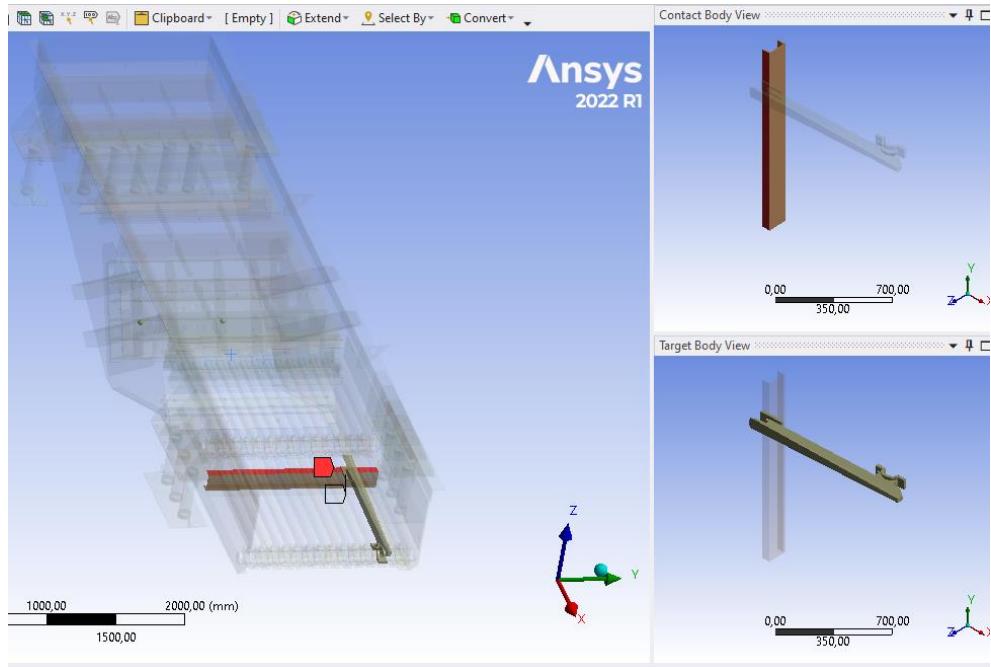


Figure 3.16 Example of contact controlling

Details of "Contact Region 564"	
Scope	
Scoping Method	Geometry Selection
Contact	1 Face
Target	1 Face
Contact Bodies	DIN1026-1 - U 140 - 1300\Solid1
Target Bodies	BT-05-0301\Solid1
Protected	No
Definition	
Type	Bonded
Scope Mode	Automatic
Behavior	Program Controlled
Trim Contact	Program Controlled
Trim Tolerance	16,351 mm
Suppressed	No
Advanced	
Formulation	Program Controlled
Small Sliding	Program Controlled
Detection Method	Program Controlled

Figure 3.17 Details about one of the contact

Mesh operation was performed after the contacts were assigned.

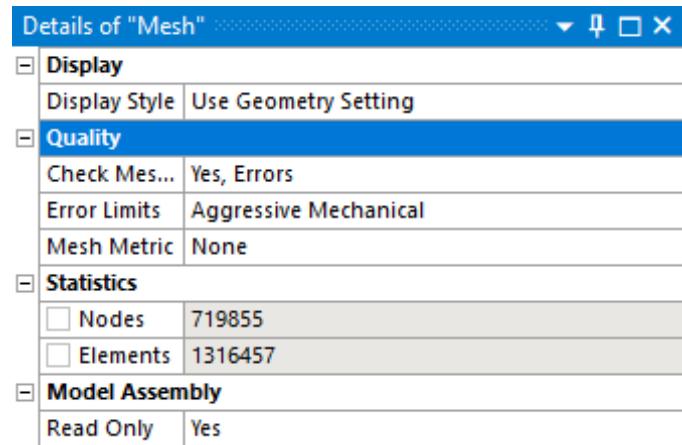


Figure 3.18 Details and options of mesh operation for the first feeder

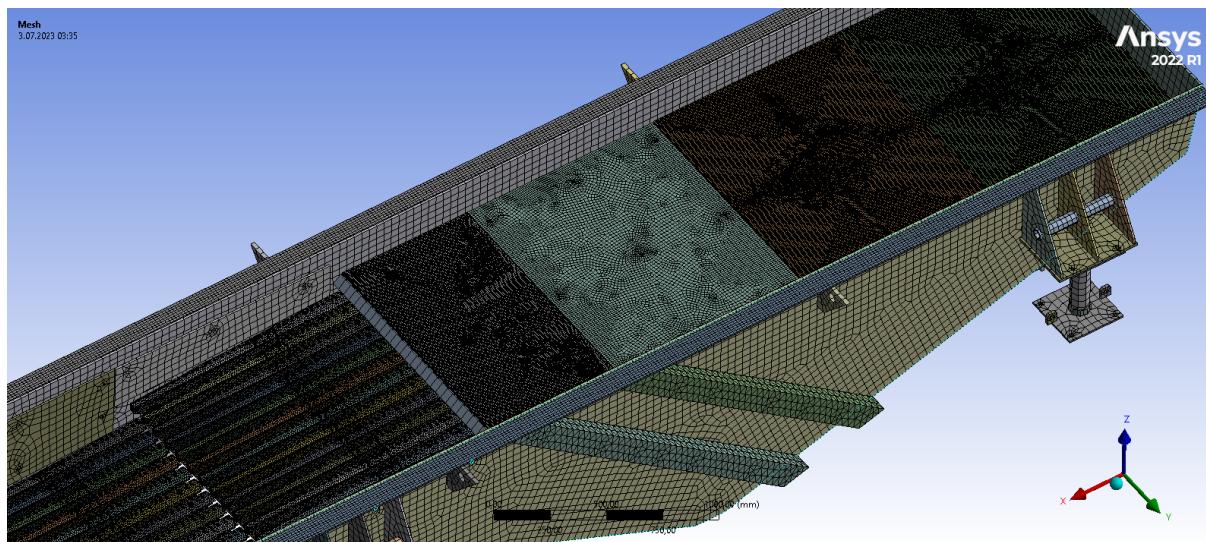


Figure 3.19 First feeder's isometric view after mesh operation

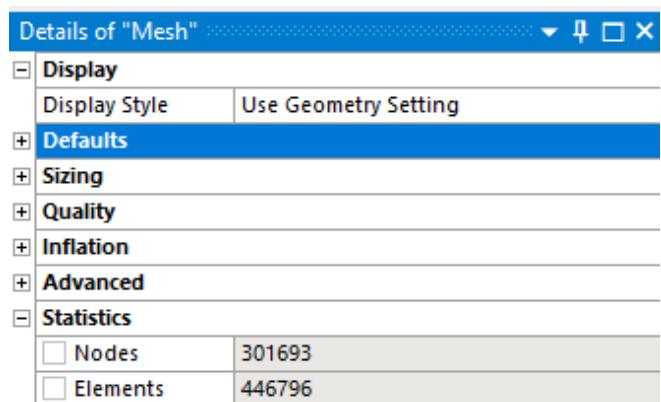


Figure 3.20 Details and options for the second feeder

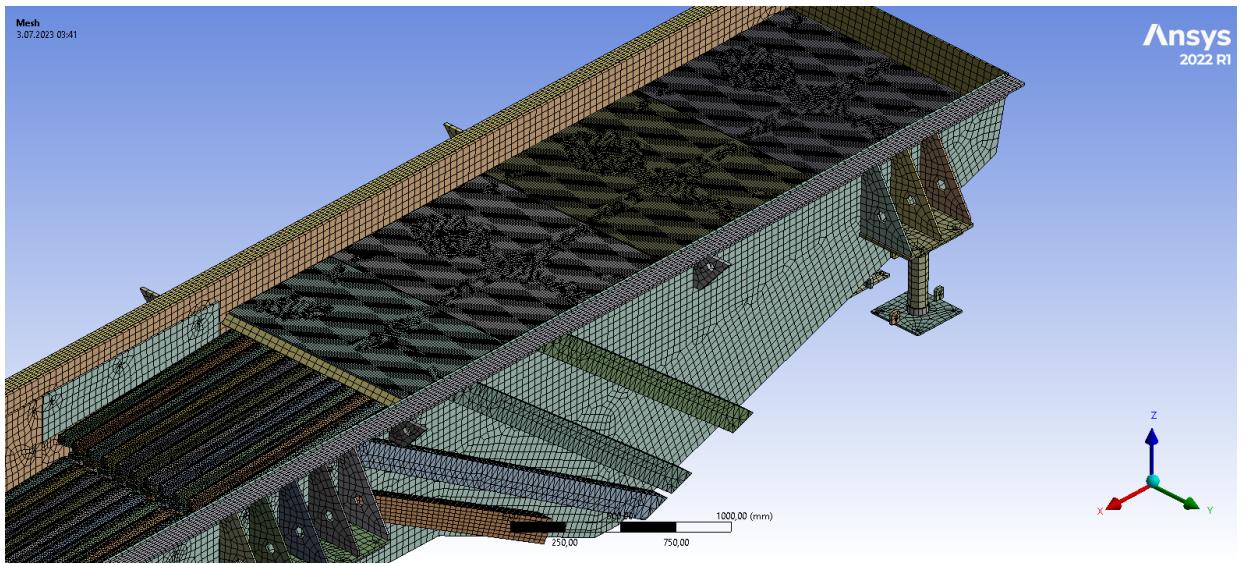


Figure 3.21 Isometric view of the second feeder after mesh operation

After the meshing process, the final preparations for the static analysis were started. First of all, in the data given by the company, a 25-ton load distributed on the feeder was added. Then, 1000 N force was added, which should act on each plate in the data specified by the company. This 1000 N was equally distributed to the stepped grilles in front of the feeders. There were 14 grids in each tier, so the force falling on each grid was assigned as 71.43 N.

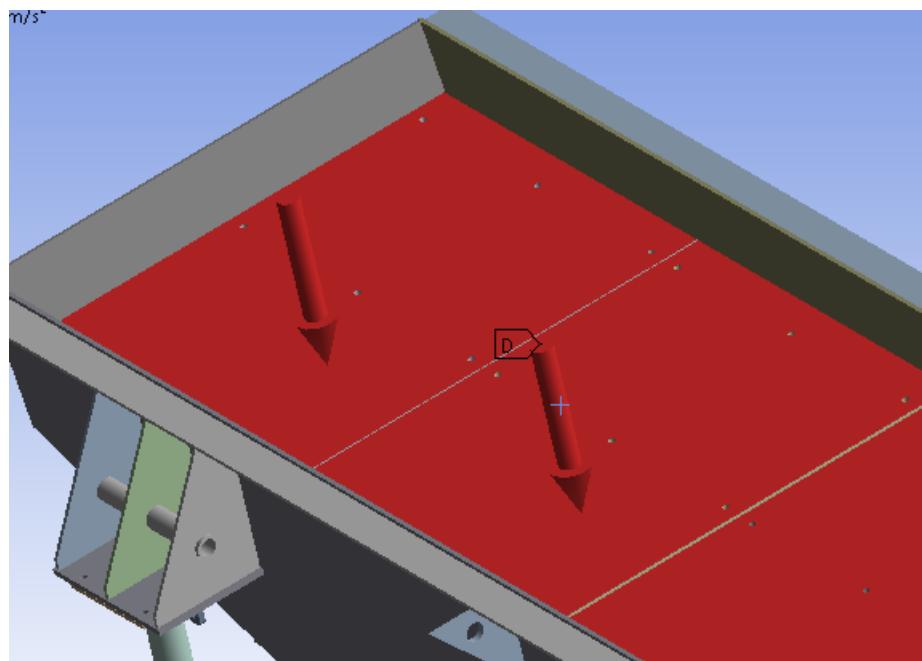


Figure 3.22 Forces of 1000 N applied to the plate.

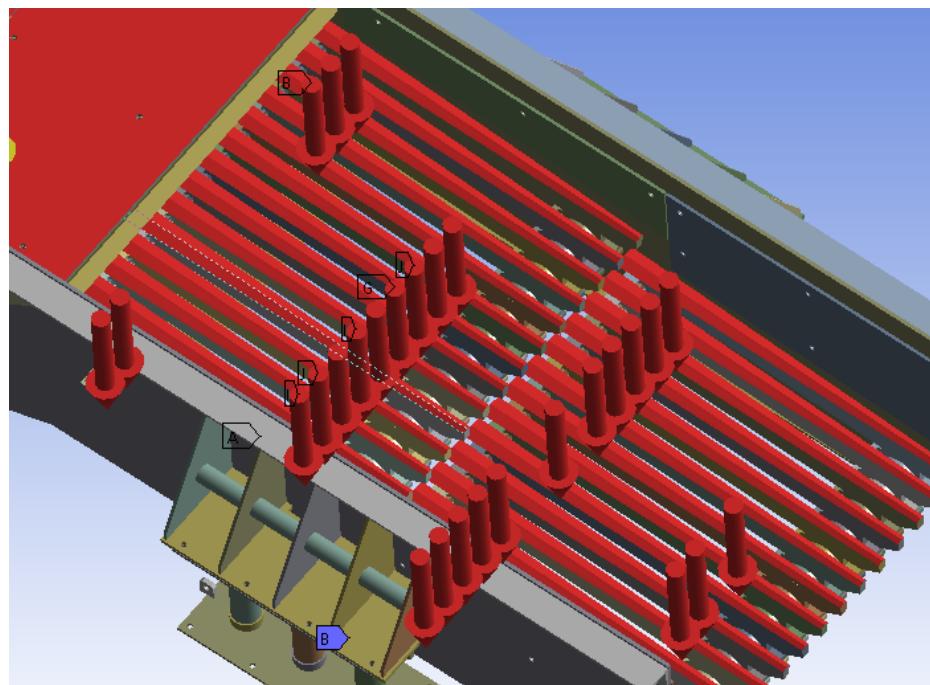


Figure 3.23 Forces of 71,43 N applied to the grids.

After these processes, the gravitational force required for the accuracy of the analysis was added.

Finally, the fixed supports required for analyzing the feeders were determined.

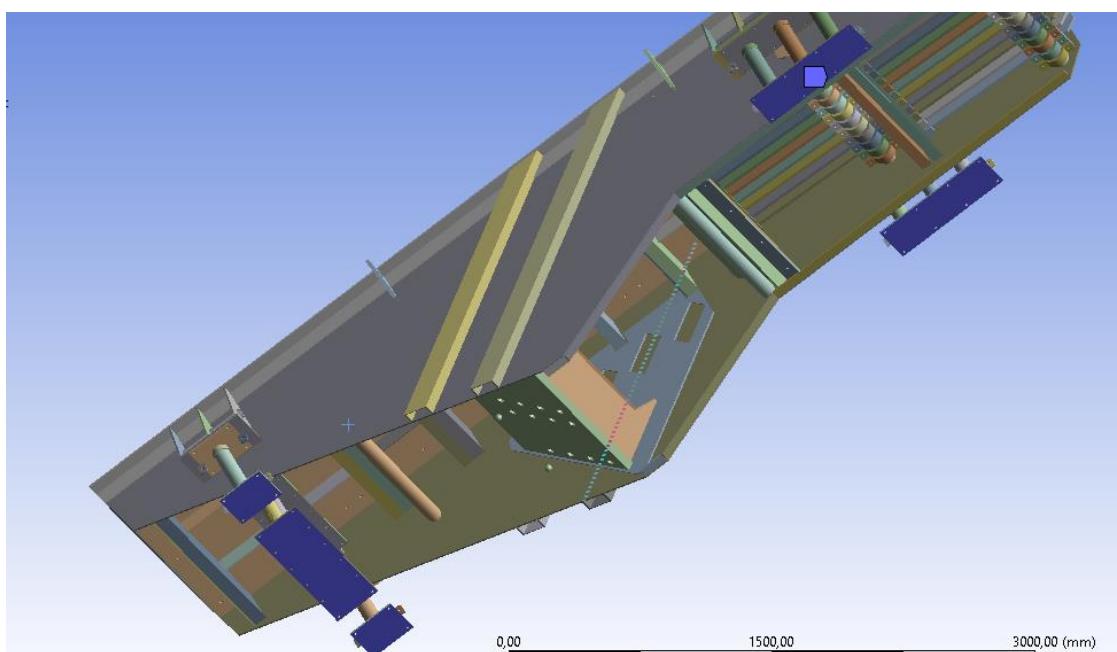


Figure 3.24 Fixed supports

3.1.2 Results of Stress Analysis

Three analyzes were performed: Total Deformation, Equivalent Elastic Strain, and Equivalent Stress.

Results of Stress Analysis for First Feeder

The Total Deformation analysis results of the first feeder are shown in the image below. Color and amount of deformation can be seen in mm on the deformation scale on the left side of the image. The highest deformation turned out to be 0.81546 mm. The average deformation was 0.30424 mm.

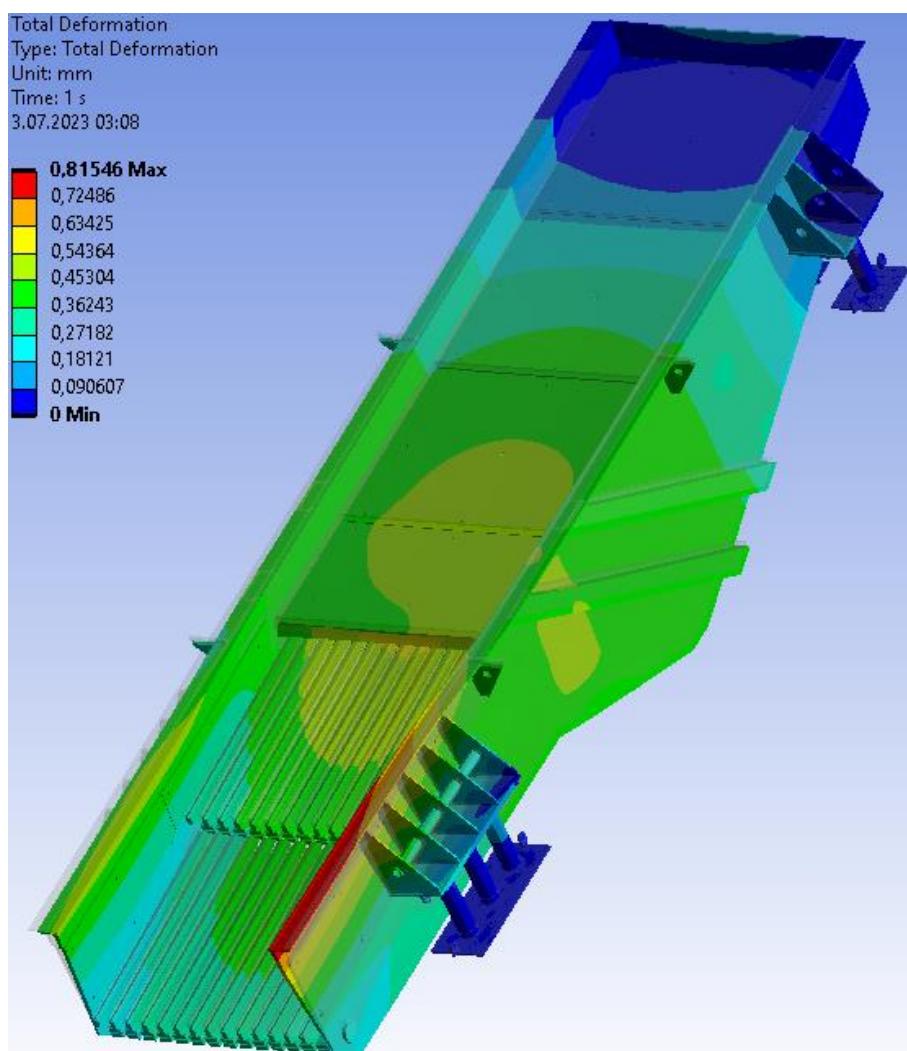


Figure 3.25 Stress analysis - total deformation for the first feeder

Figure 3.26 shows the Equivalent Elastic Strain analysis result of the first feeder. As a result of the analysis, the highest Equivalent Elastic Strain is obtained as 0.00095472. The lowest Equivalent Elastic Strain value is 0.0000000013396.

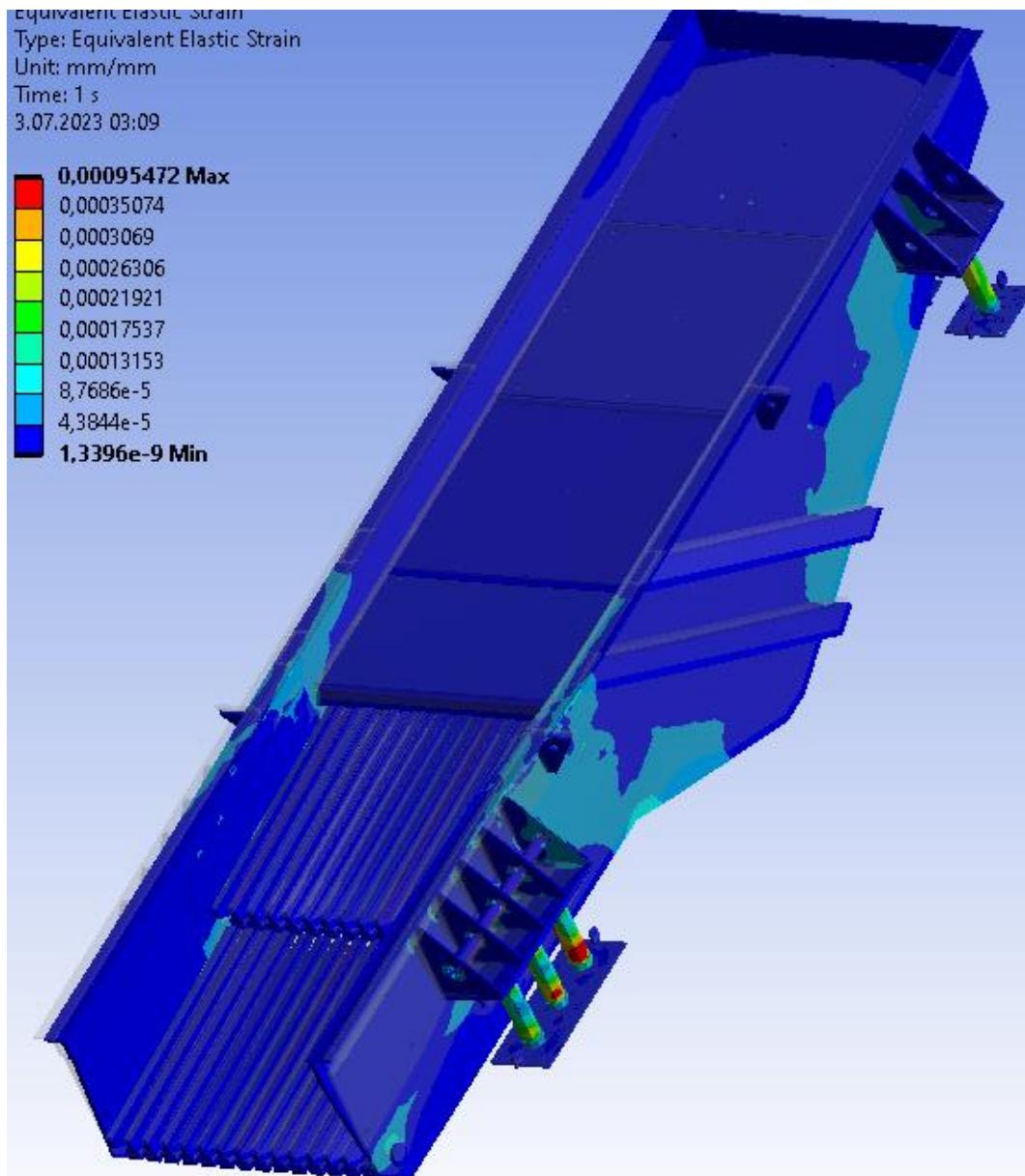


Figure 3.26 Stress analysis - equivalent elastic strain for the first feeder

In Figure 31, there is the Equivalent (von-Mises) Stress analysis result, which is the last analysis result of the first feeder. As a result of the analysis, the highest Equivalent (von-Mises) Stress is 164.84 MPa. The lowest Equivalent (von-Mises) Stress value is 0.00014889 MPa.

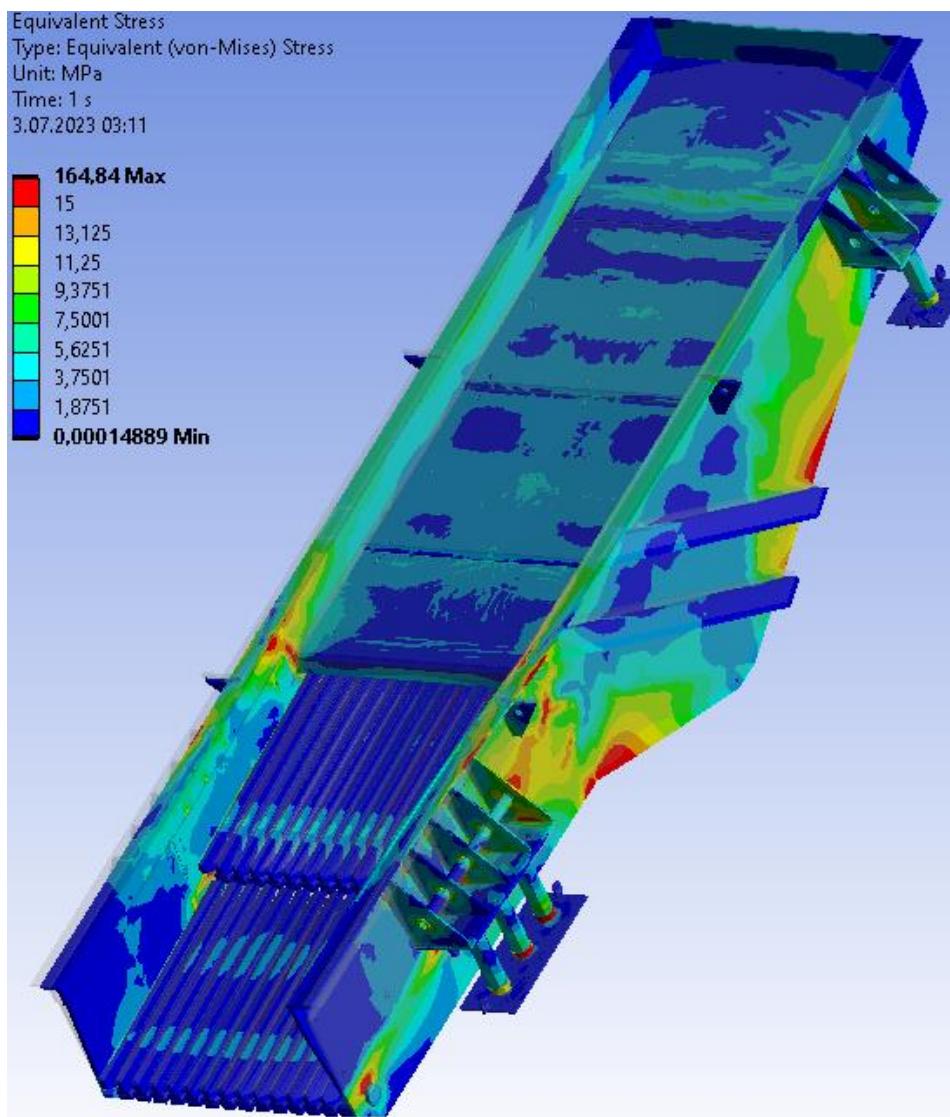


Figure 3.27 Stress analysis - equivalent (von-Mises) stress for the first feeder

Results of Stress Analysis for Second Feeder

The figure below shows the Total Deformation analysis result of the second feeder in mm. As a result of the analysis, the highest Total Deformation value was 0.72476 mm. The lowest total deformation value is 0 mm. In other words, there are points where deformation does not occur.

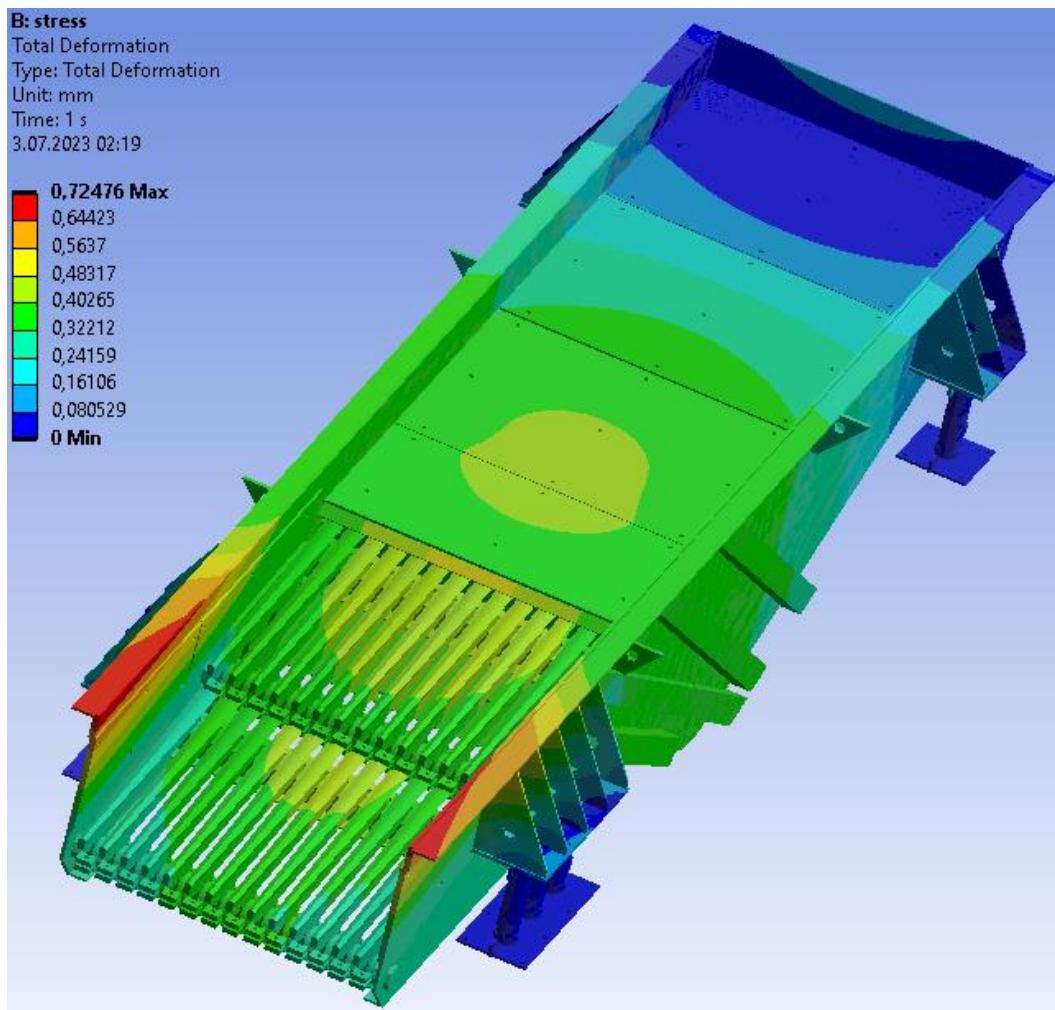


Figure 3.28 Stress analysis - total deformation for the second feeder

The figure below depicts the Equivalent Elastic Strain analysis result of the second feeder. As a result of the analysis, the highest Equivalent Elastic Strain is obtained as 0.00087525. The lowest Equivalent Elastic Strain value is 0.00000001707.

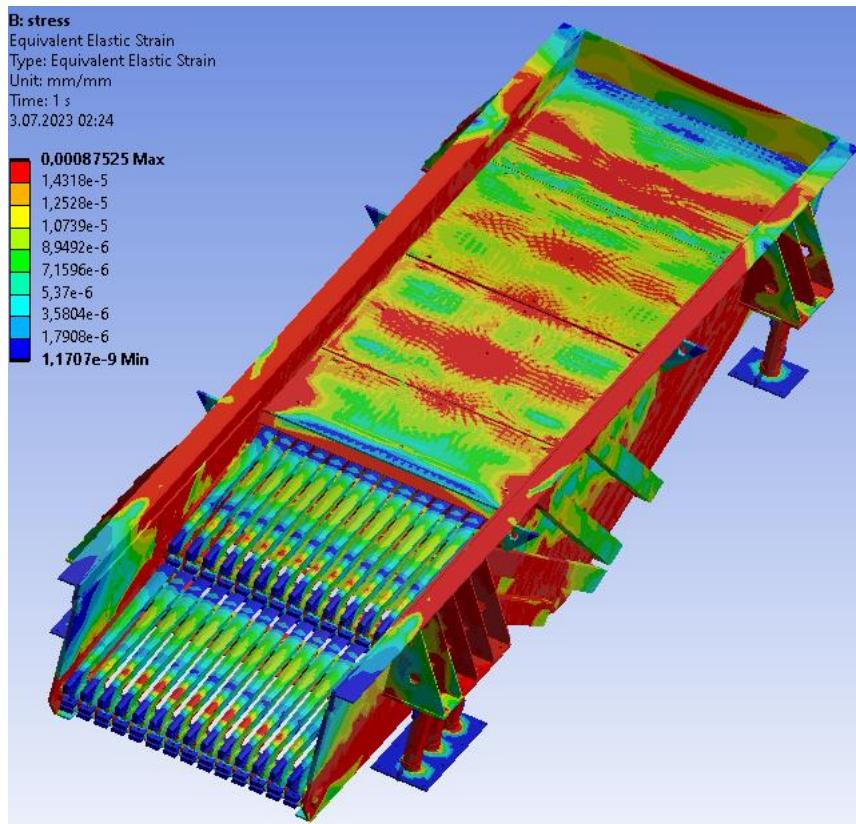


Figure 3.29 Stress analysis - equivalent elastic strain for the second feeder

In the figure below is the Equivalent (von-Mises) Stress analysis result, which is the last analysis result of the second feeder. As a result of the analysis, the highest Equivalent (von-Mises) Stress is 136 MPa. The lowest Equivalent (von-Mises) Stress value is 0.00010067 MPa. The color scale has been expanded as very few places have high stress.

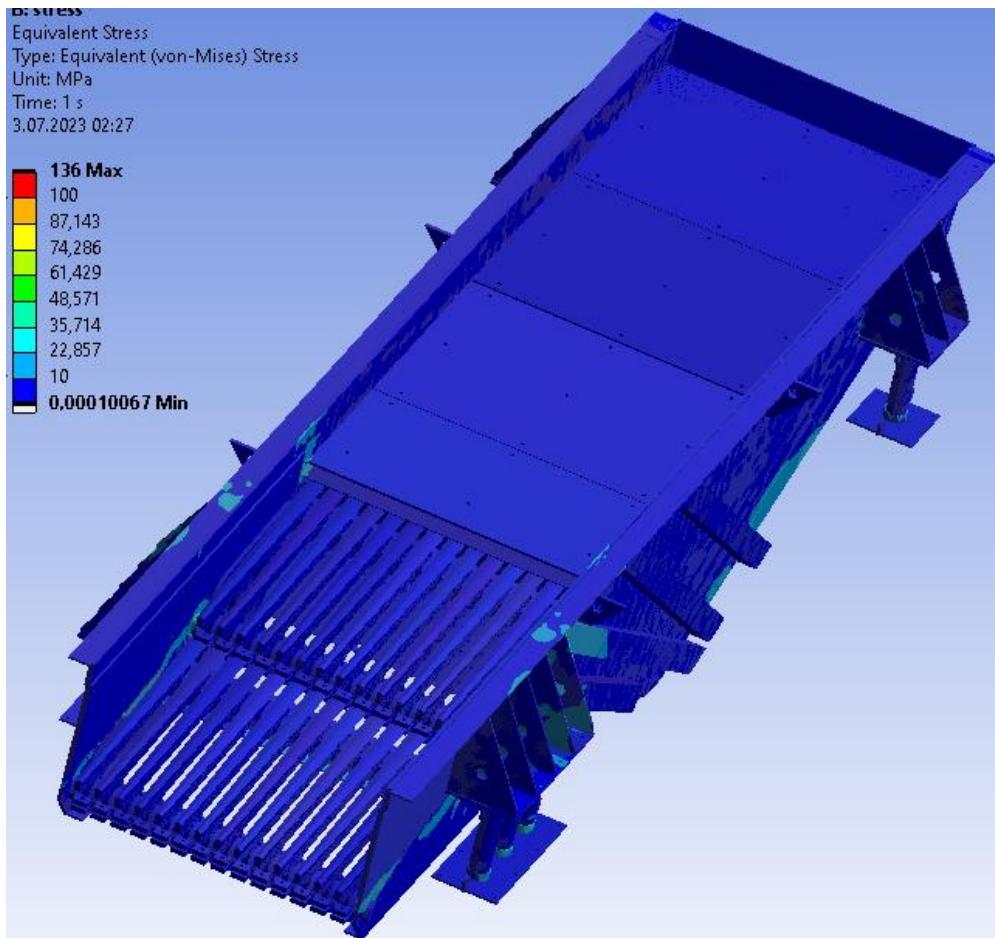


Figure 3.30 Stress analysis - equivalent (von-Mises) stress for the second feeder

3.2 Vibration Analysis

3.2.1 Preparation for Vibration Analysis

As in stress analysis, some preliminary preparations need to be made for vibration analysis. These preparations are essential for accurate and error-free vibration analysis.

Again, as in the stress analysis, the preparation steps for both feeders are the same. First of all, the modal block should be created via ANSYS Workbench. After creating this block, the Model in the block used in Stress Analysis and the model created for the modal are linked. In this way, the same transactions are not repeated, thus saving work and time (Xueqin and Xiaoming, 2008).

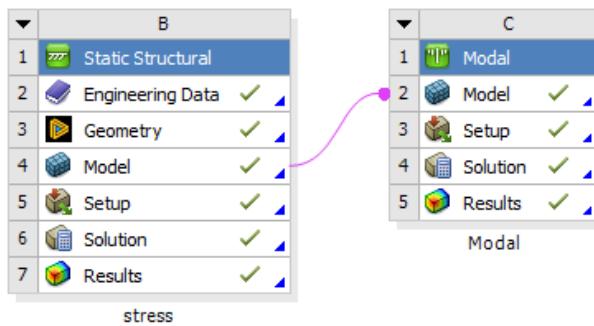


Figure 3.31 Connecting static structural's model to modal's model

After this process, ANSYS Mechanical opens in the Modal block. Fixed supports are determined from the same places as in the stress analysis. It is entered in the Analysis Settings tab. The "Max Modes to Find" option is set to 50 to get more detailed results from here.

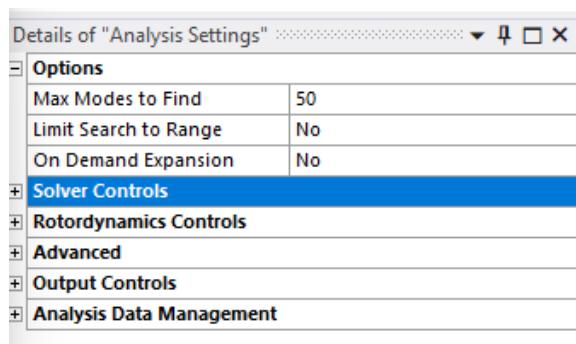


Figure 3.32 Analysis setting tab

After this process is done, this project is saved and returned to ANSYS Workbench. The Response Spectrum block required for Vibration Analysis in ANSYS Workbench is added. Then, as in Modal, the Model in Modal and the Model in Response Spectrum are connected; It connects with Solution in Modal and Setup in Response Spectrum (Yongfeng et al., 2005).

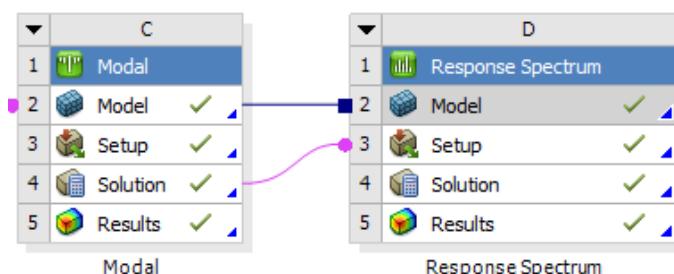


Figure 3.33 Connecting modal's solution to response spectrum's setup

Then RS Displacement is added to the Response Spectrum tab. In RS Displacement, the

frequency information of the motor is entered. The same motors are used for both feeders analyzed. The frequency of the motors was checked from the document sent by the company and entered as 50 Hz.



MVE 19500/1E-105A0 [EE619500A5A08A0000]
3 PH - 6 kutup - 1000 d/d - 380-415 V [Delta] - 50 Hz

Figure 3.34 Frequency data of the engine

3.2.2 Results of Vibration Analysis

In the results of Vibration Analysis, three analysis results were examined, namely Equivalent Stress, Total Deformation and Normal Elastic Strain.

3.2.2.1 Results of Vibration Analysis for First Feeder

The final report of Equivalent Stress is given in the image below. The highest Equivalent Stress value was 856.59 MPa.

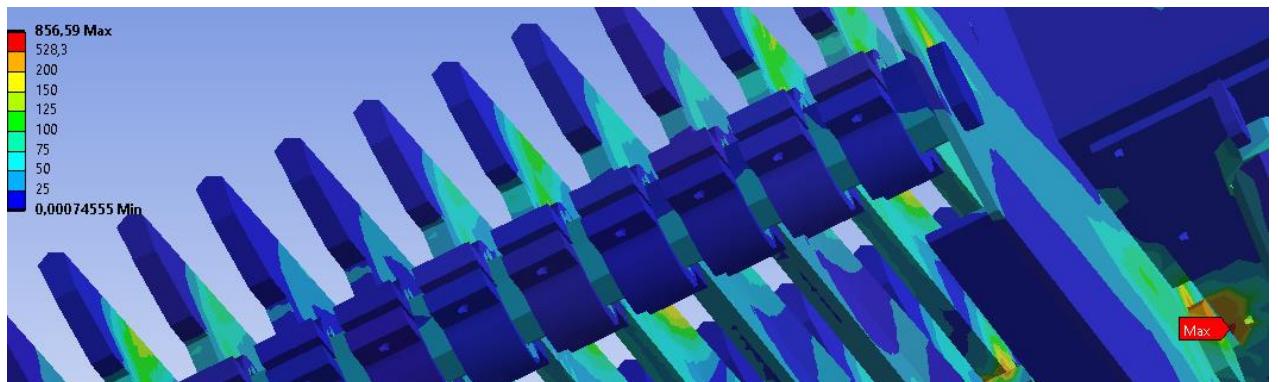


Figure 3.35 Vibration Analysis - Equivalent Stress critical areas for the first feeder

The minimum Equivalent Stress value was 0.00074555 MPa. The average Equivalent Stress value was 21.4 MPa.

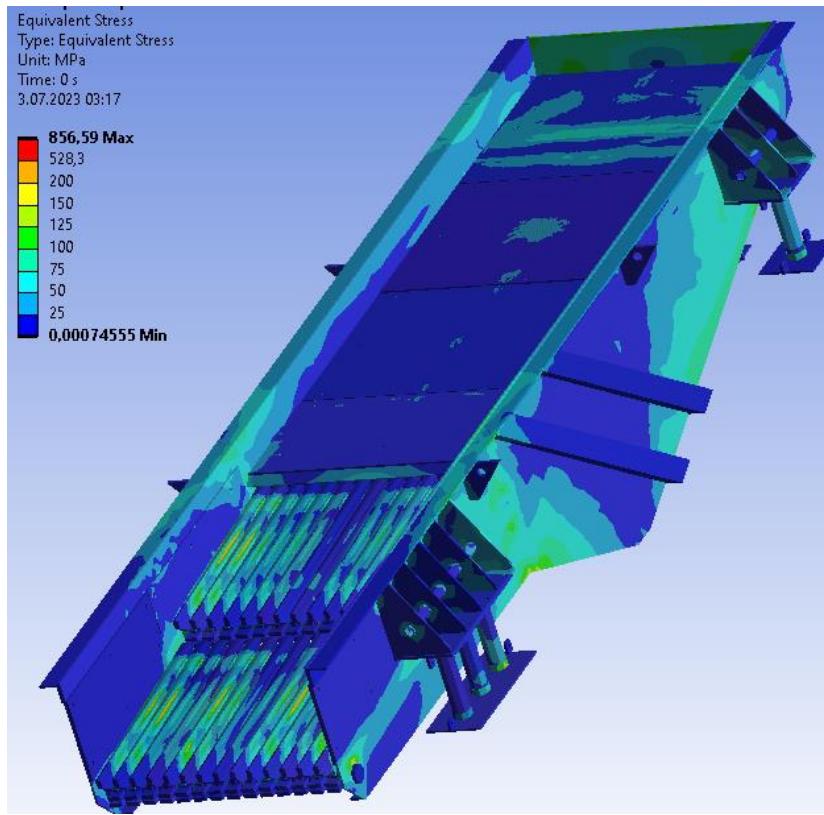


Figure 3.36 Vibration Analysis - Equivalent Stress for the first feeder

The deformation results at 50 Hz are given in the image below.

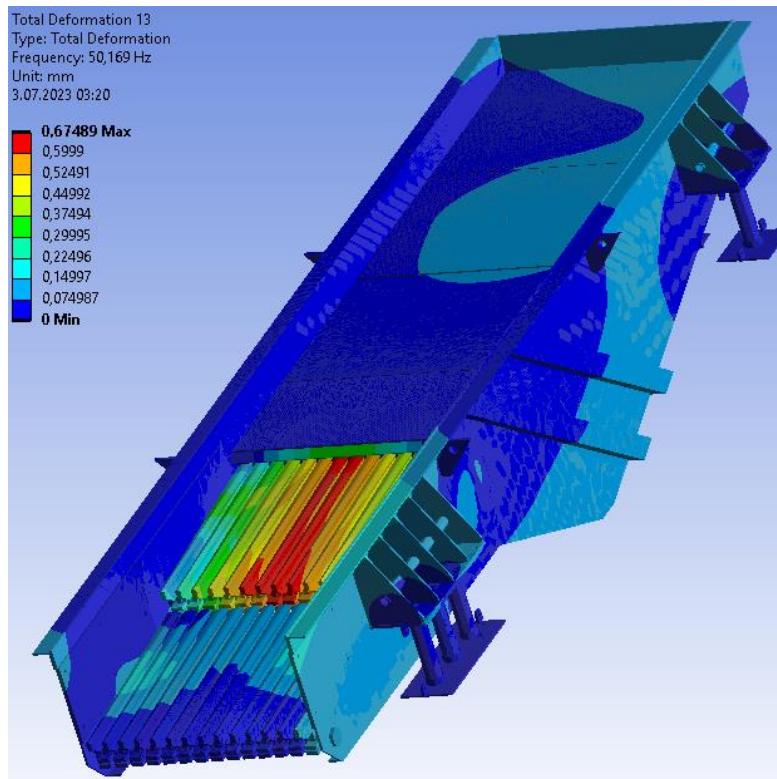


Figure 3.37 Vibration Analysis - Total Deformation at 50,169 Hz for the first feeder

After Equivalent Stress results, Total Deformation results were passed. The deformation amounts here are given in mm. As a result of the analysis, the highest deformation amount was 4.7285 mm. The lowest deformation value is 0. In other words, there are points with no deformation in the feeder.

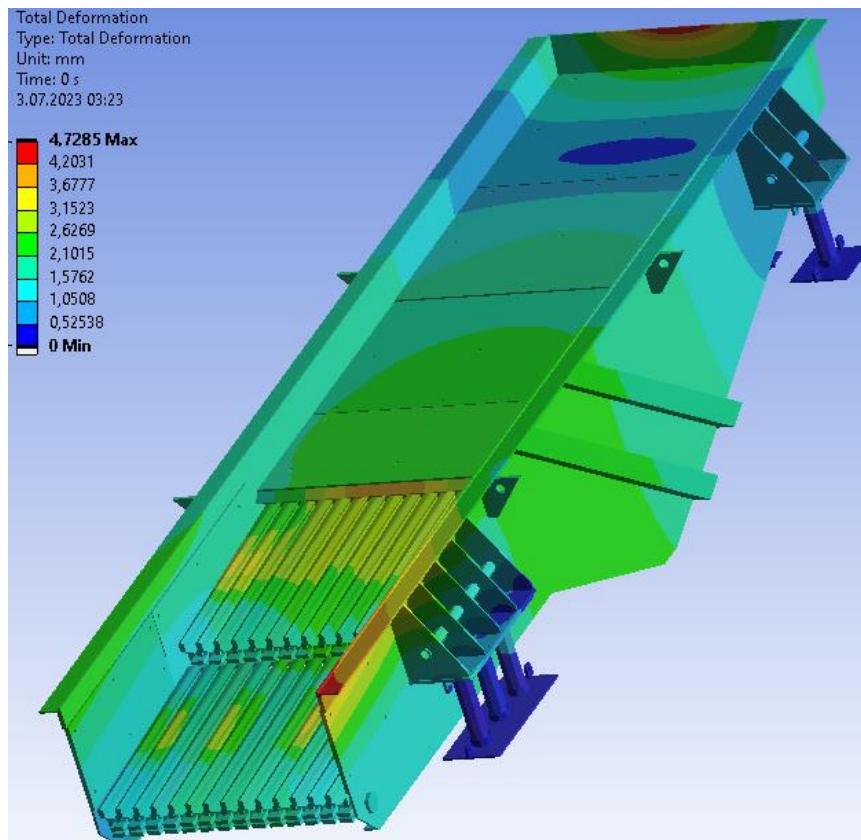


Figure 3.38 Vibration Analysis - Total Deformation of the first feeder

The last vibration analysis result of the first feeder is Normal Elastic Strain. The highest strain amount is 0.0014742 and the lowest strain amount is $4,7444 \times 10^{-21}$.

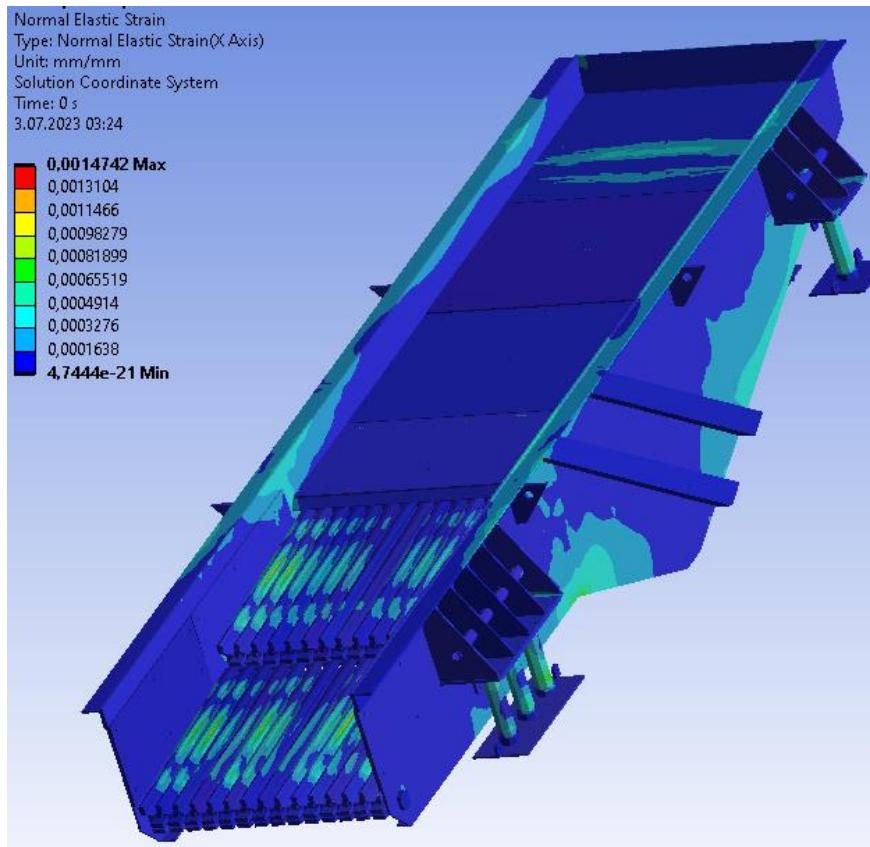


Figure 3.39 Vibration Analysis - Normal Elastic Strain on X Axis for first feeder

3.2.2.2 Results of Vibration Analysis for Second Feeder

The final report of Equivalent Stress is given in the image below. The highest Equivalent Stress value was 505.4 MPa.

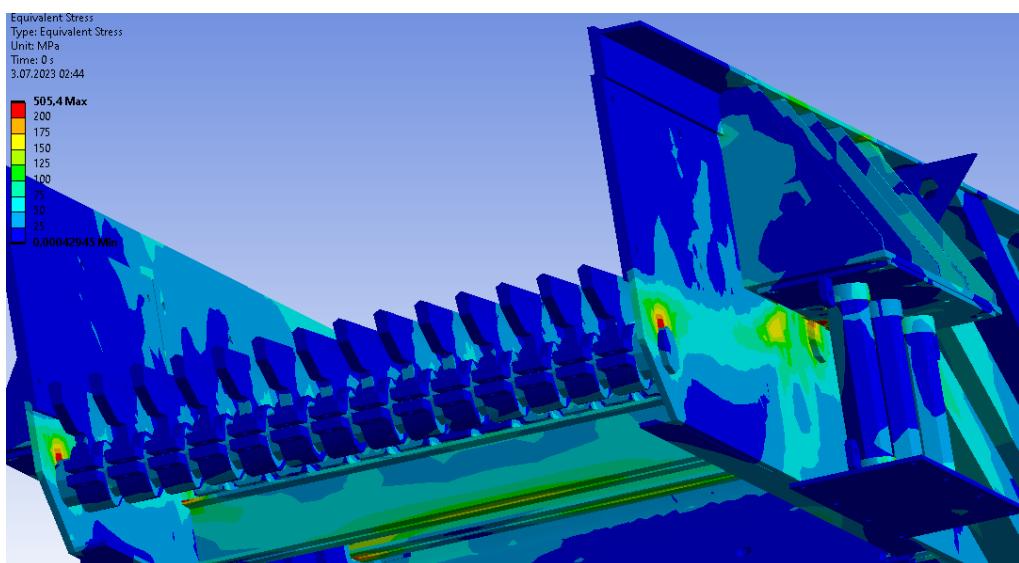


Figure 3.40 Vibration Analysis - Equivalent Stress Red Areas for the second feeder

The minimum Equivalent Stress value is 0.00042945 MPa. The average Equivalent Stress value is 22.893 MPa.

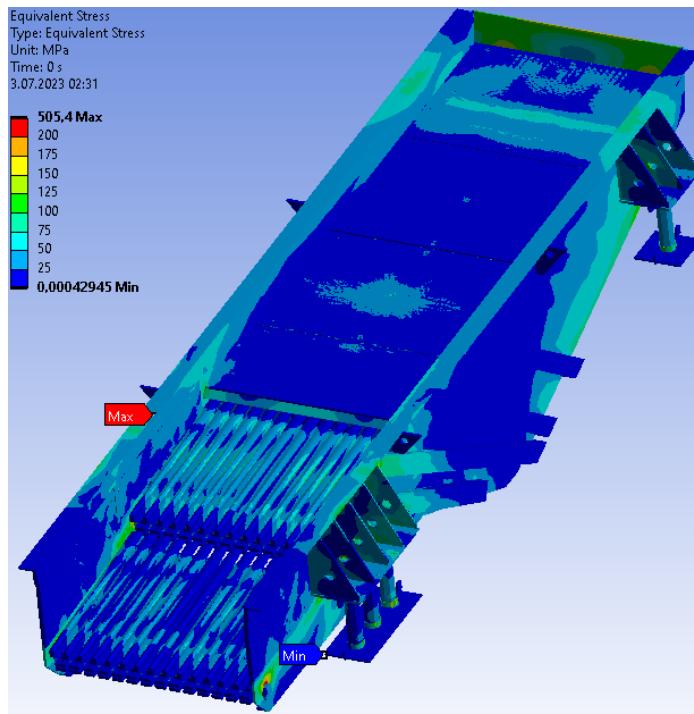


Figure 3.41 Vibration Analysis - Equivalent Stress for the second feeder

After Equivalent Stress results, Total Deformation results were passed. The deformation amounts here are given in mm. As a result of the analysis, the highest deformation amount was 5,9846 mm. The lowest deformation value is 0. In other words, there are points with no deformation in the feeder.

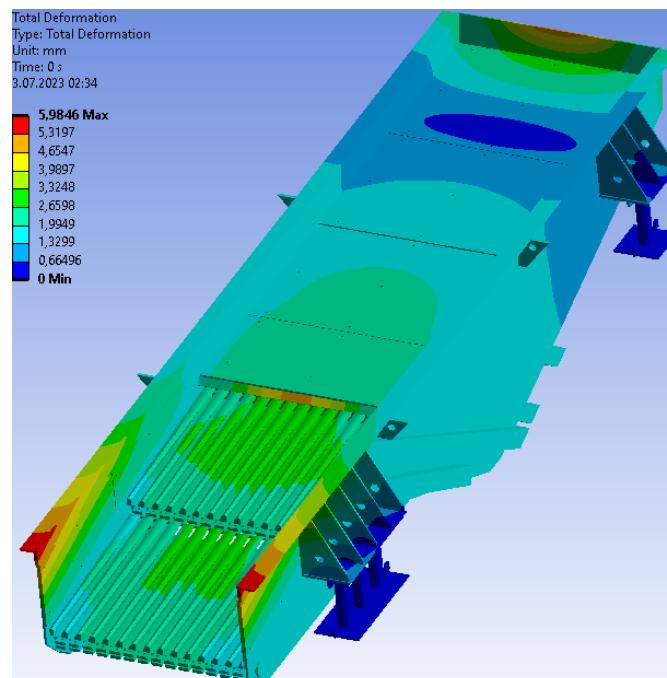


Figure 3.42 Vibration Analysis - Total Deformation for the second feeder

The deformation results at 50 Hz are given in the image below.

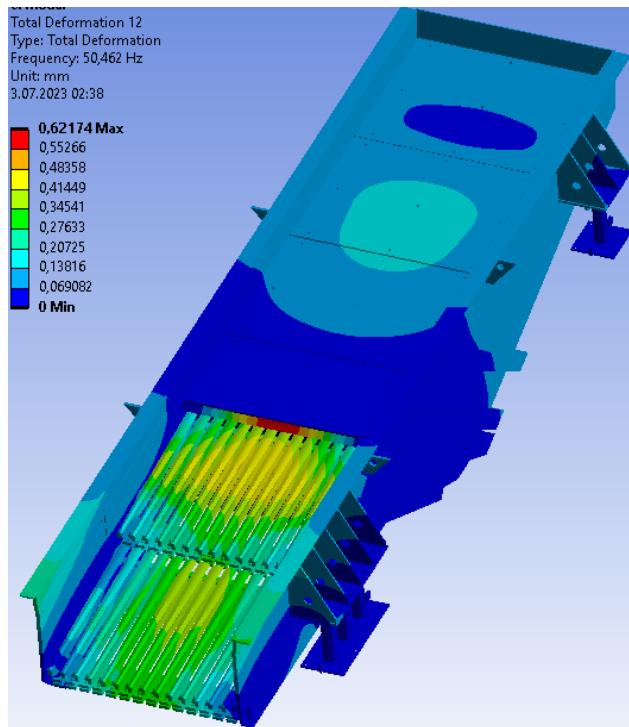


Figure 3.43 Vibration Analysis - Total Deformation at 50,462 Hz of the second feeder

The last vibration analysis result of the second feeder is Normal Elastic Strain. The highest strain amount is 0.0019076 and the lowest strain amount is 2.9017×10^{-10} .

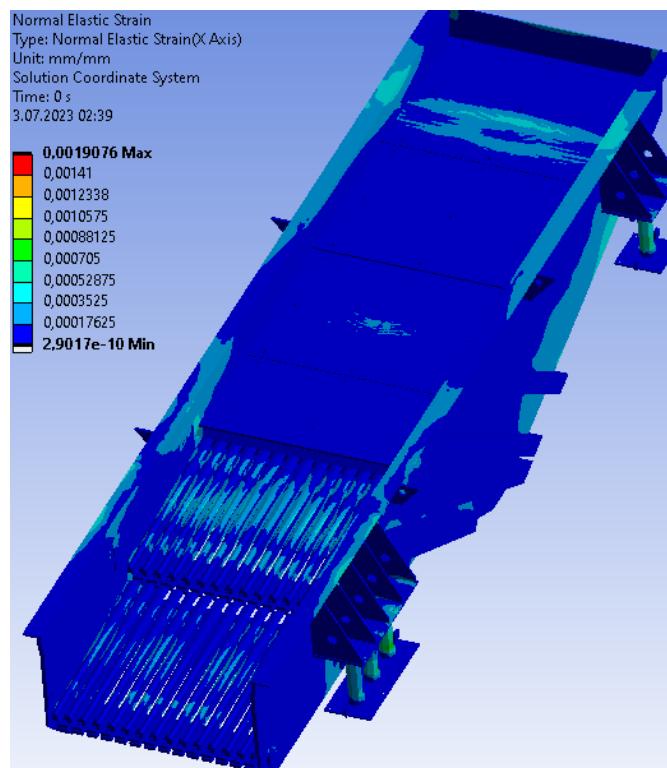


Figure 3.44 Vibration Analysis - Normal Elastic Strain on X Axis for second feeder

3.3 Fatigue Analysis

3.3.1 Preparation for Fatigue Analysis

There are also preparations to be made for Fatigue Analysis. These preparations are essential for Fatigue Analysis results to be accurate and error-free.

The Fatigue Tool must be used for Fatigue Analysis. The Fatigue Tool can be selected in the Static Structural block. The Static Structural block is assigned to the model in the Response Spectrum for evaluation along with the vibration analysis. So a new Static Structural block is created, linked to the model in the Response Spectrum.

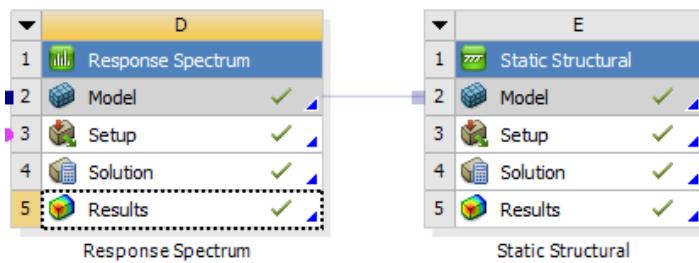


Figure 3.45 Connecting response spectrum's model to static structural's model

ANSYS Mechanical is opened by right-clicking on the Setup option in the Static Structural block in ANSYS Workbench and added to Fatigue Tool Solution. The results needed in the Fatigue Tool are added to the tree. Life, Damage and Safety Factor has been added to the Fatigue Tool results in this analysis (Li et al., 2008).

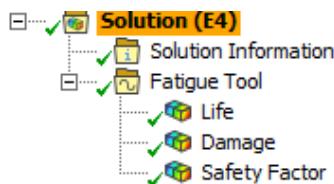


Figure 3.46 Fatigue Tool

The same preparatory procedures required for the Static Structural here were performed as in the Stress Analysis. However, since the Model is bound, there was no need to do some operations again. A force of 1000N was defined separately for each plate. A force of 71.43 N was defined for each of the 14 grids on the first floor. Forces of 71.43 N were then defined for each of the 14 grids on the second floor. Standard Earth Gravity is defined. Fixed Supports were defined as in Stress Analysis.

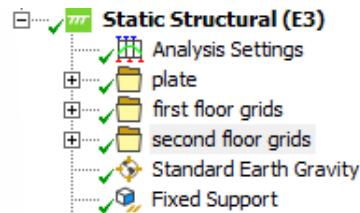


Figure 3.47 Static preparations for fatigue analysis

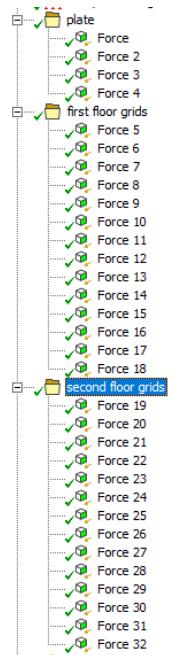


Figure 3.48 Grouping of forces

3.3.2 Results of Fatigue Analysis

As mentioned before, Life, Damage and Safety Factor analysis results will be examined.

3.3.2.1 Results of Fatigue Analysis for First Feeder

The result of the life analysis is given in the image below.

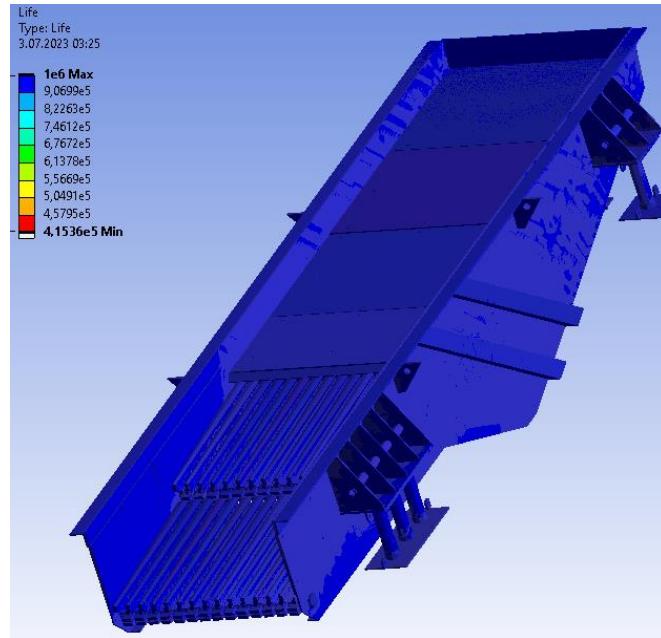


Figure 3.49 Fatigue Analysis - Life for the first feeder

The point with the minimum value of the Life analysis is as follows:

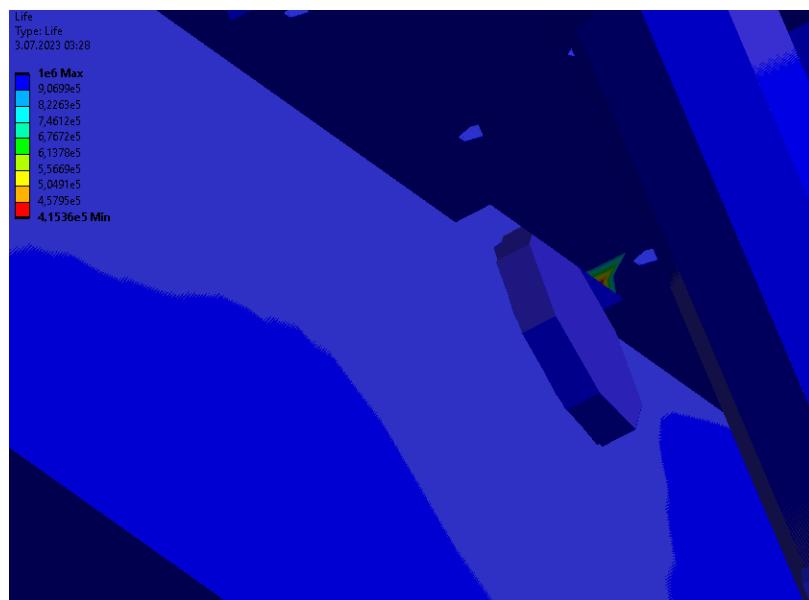


Figure 3.50 Fatigue Analysis - Life critical point for the first feeder

The result of the damage analysis is given in the figure below.

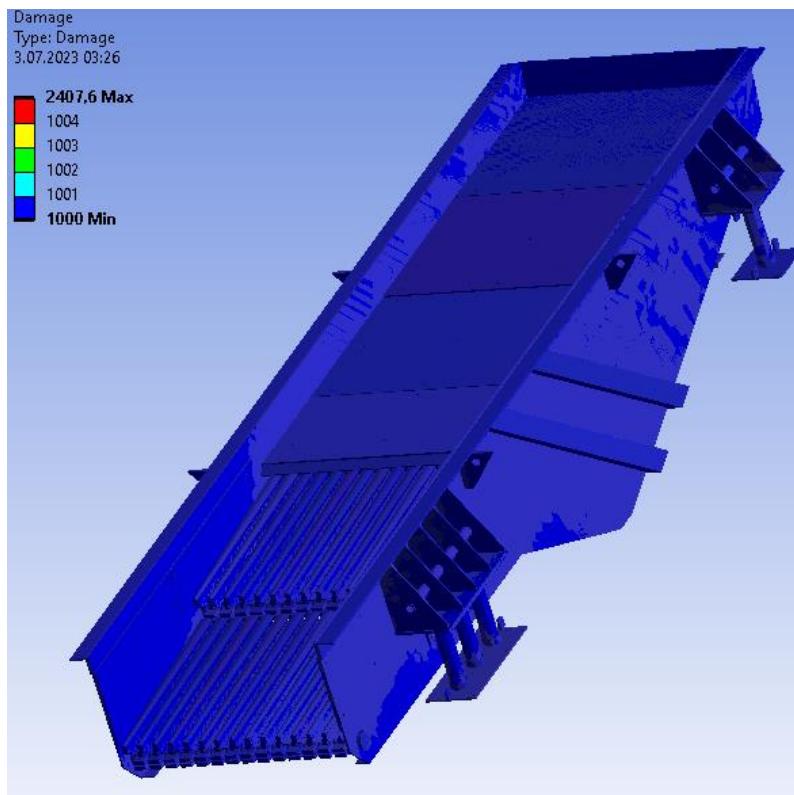


Figure 3.51 Fatigue Analysis - Damage for first feeder

The point with the highest result of the damage analysis is given in the figure below.

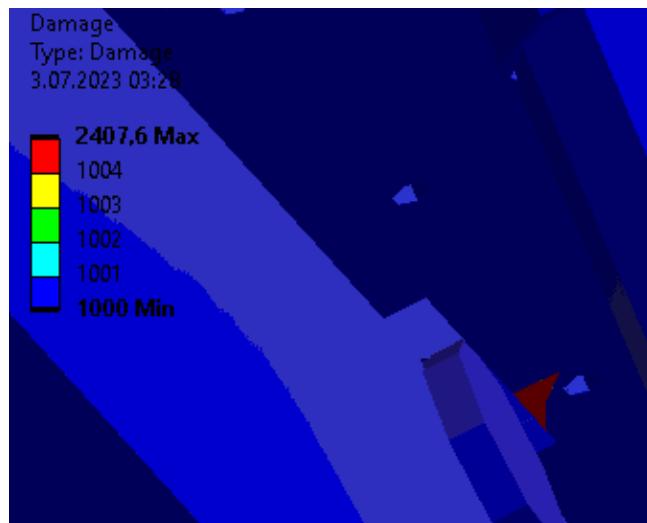


Figure 3.52 Fatigue Analysis - Damage red area for the first feeder

The result of the Safety Factor Analysis is given in the figure below. The location of the plates is not shown in the image because they are dark blue in color; that is, they have the

maximum safety factor value.

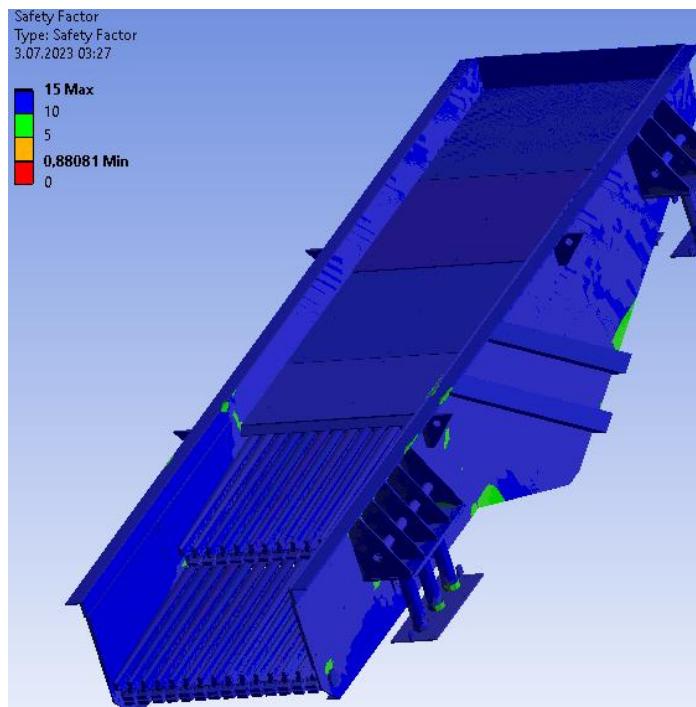


Figure 3.53 Fatigue Analysis - Safety Factor for the first feeder

3.3.2.2 Results of Fatigue Analysis for Second Feeder

The result of the life analysis is given in the image below.

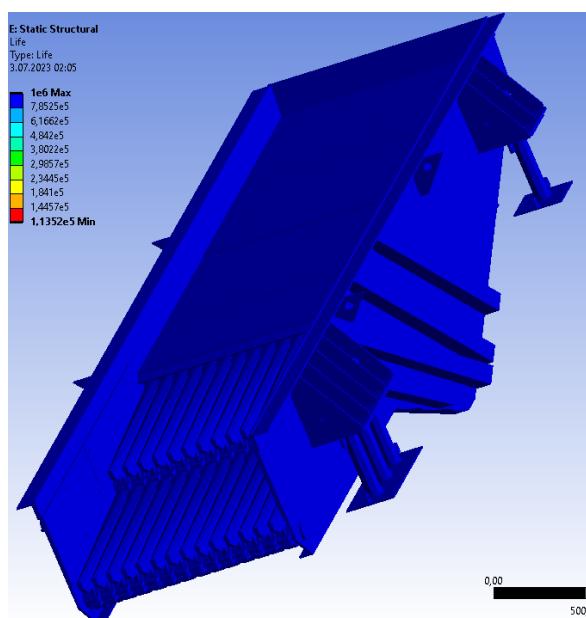


Figure 3.54 Fatigue Analysis - Life for the second feeder

The result of the damage analysis is given in the figure below.

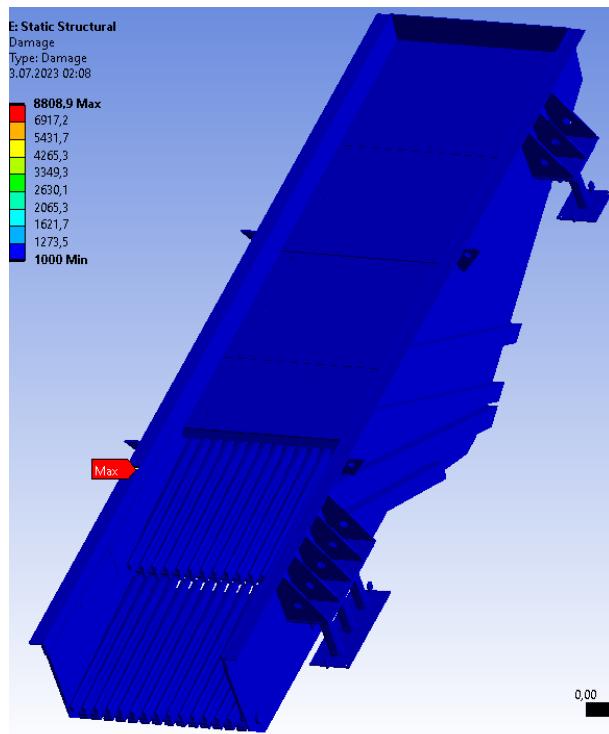


Figure 3.55 Fatigue Analysis - Damage for the second feeder

The result of the Safety Factor Analysis is given in the figure below. The location of the plates is not shown in the image because they are dark blue in color; that is, they have the maximum safety factor value.

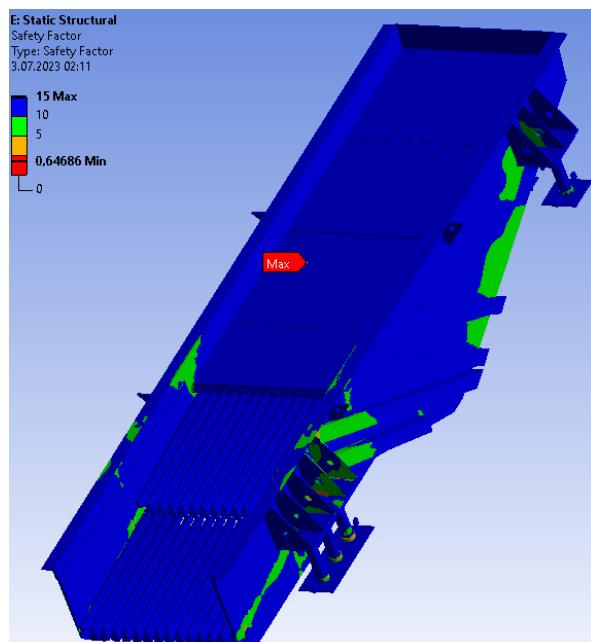


Figure 3.56 Fatigue Analysis - Safety Factor for the second feeder

3.4 Analysis of Critical Frequencies

After the analysis, the deformations at critical frequencies for both feeders were examined. The six frequency values in which the deformations appear most clearly as a result of the analyzes for both feeders are given in the figures below. The reason they are up to 50 Hz is that the motor operates at 50 Hz. (Chandrvanshi and Mukhopadhyay, 2017)

3.4.1 Total Deformations for First Feeder at Critical Frequencies

There are total the deformations for first feeder at critical frequencies:

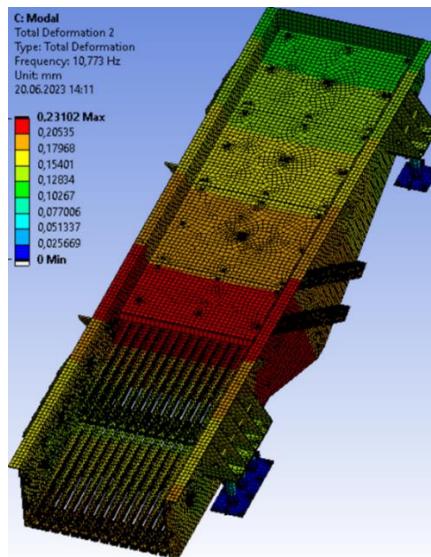


Figure 3.57 Total deformation of first feeder at 10,773 Hz

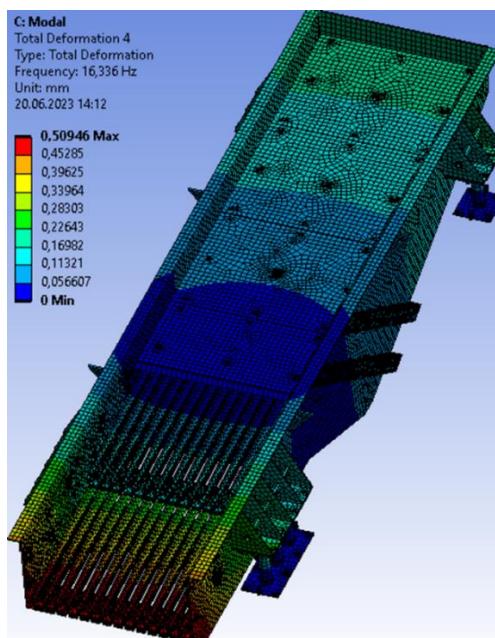


Figure 3.58 Total deformation of first feeder at 16,336 Hz

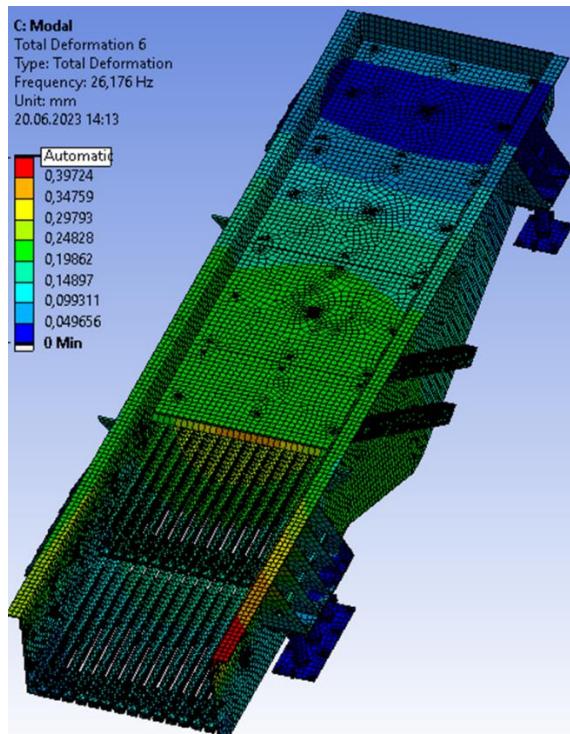


Figure 3.59 Total deformation of the first feeder at 26,176 Hz

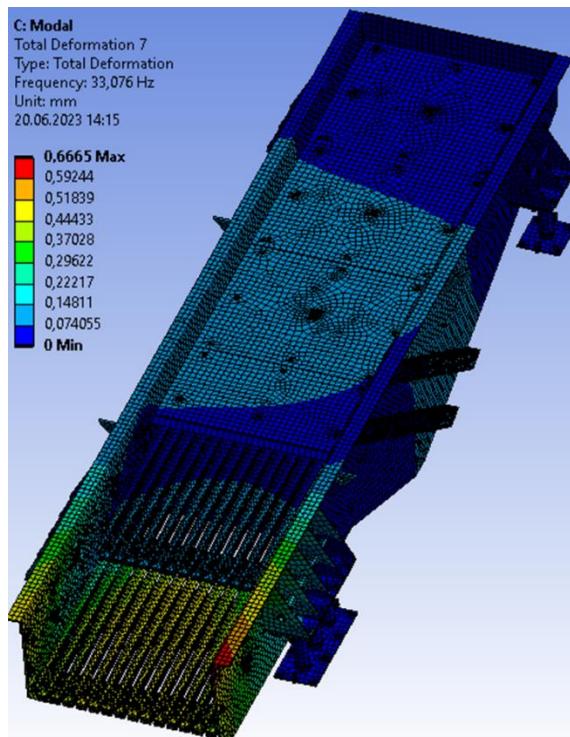


Figure 3.60 Total deformation of first feeder at 33,076 Hz

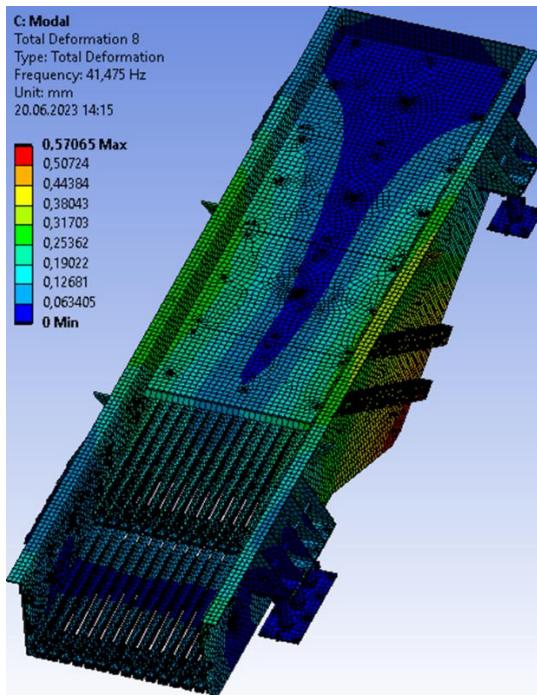


Figure 3.61 Total deformation of first feeder at 41,475 Hz

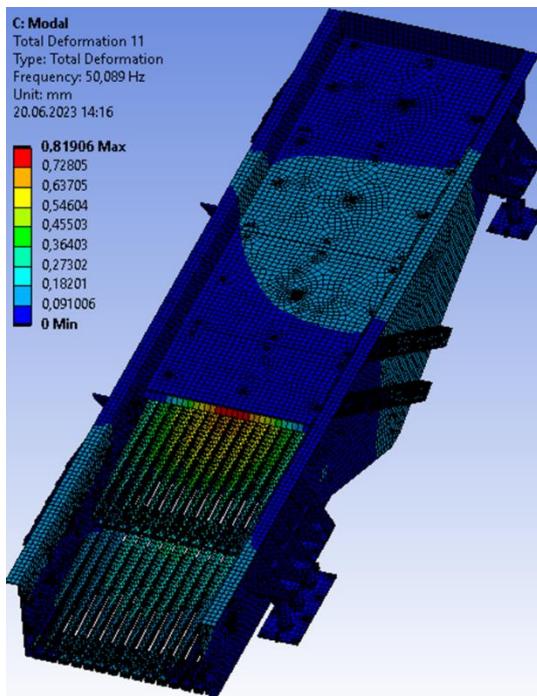


Figure 3.62 Total deformation of first the feeder at 50,089 Hz

3.4.2 Total Deformations of Second Feeder at Critical Frequencies

There are total deformations for second feeders at critical frequencies:

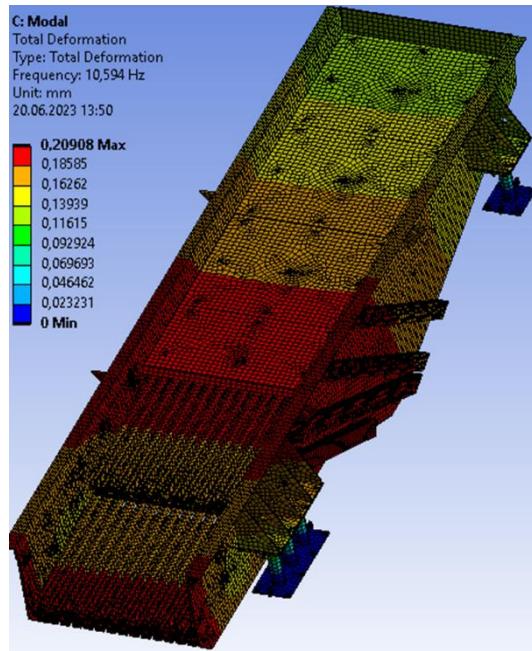


Figure 3.63 Total deformation of second feeder at 10,594 Hz

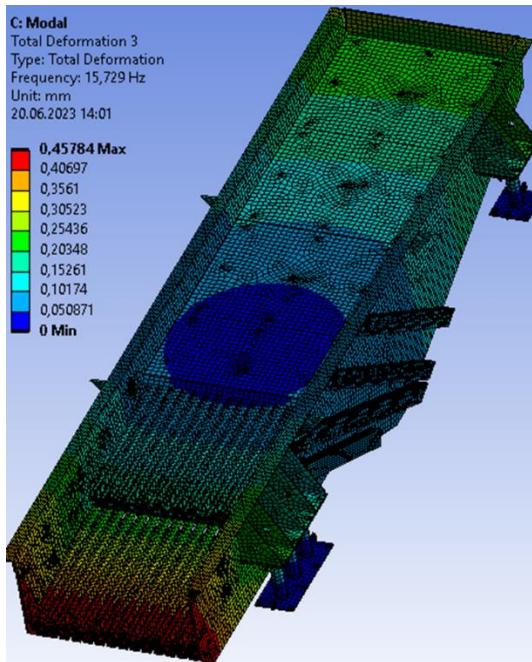


Figure 3.64 Total deformation of second feeder at 15,729 Hz

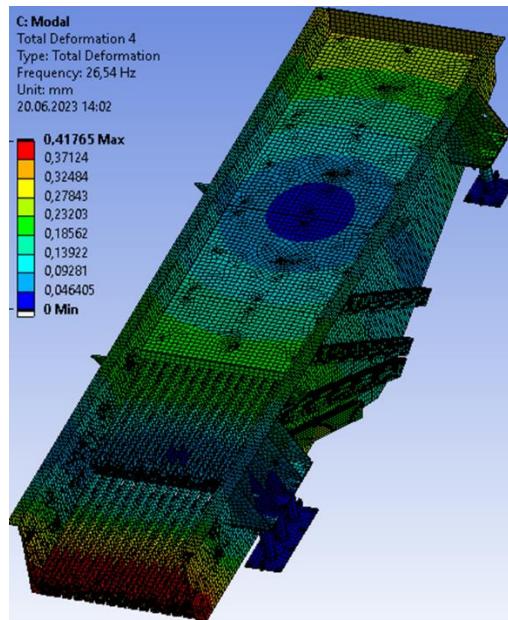


Figure 3.65 Total deformation of the second feeder at 26,54 Hz

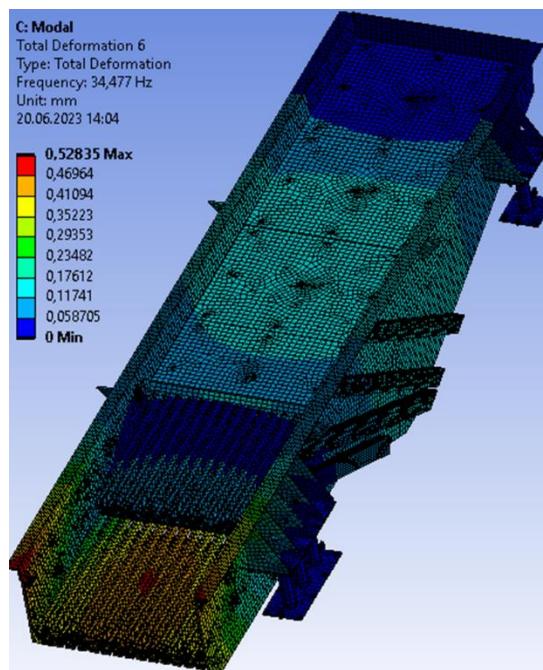


Figure 3.66 Total deformation of second feeder at 34,477 Hz

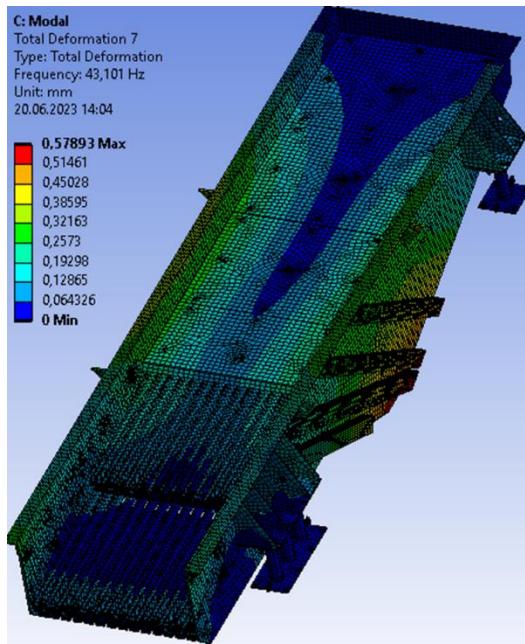


Figure 3.67 Total deformation of second feeder at 43,101 Hz

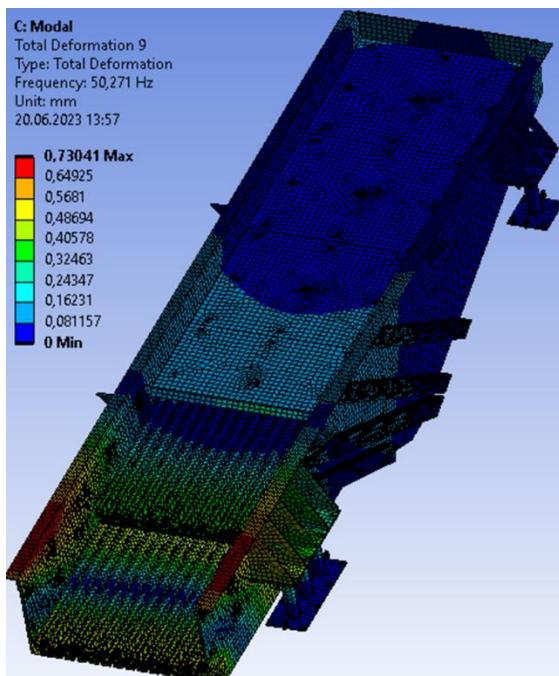


Figure 3.68 Total deformation of the second feeder at 50,271 Hz

3.5 Effect of Meshing Process on Analysis

Before performing operations in 3.1, 3.2, and 3.3, these analyses were performed with meshing with fewer nodes and elements. Then, the system was developed, and more detailed meshing was possible. More accurate results were obtained with more detailed meshing.

In addition to the number of nodes and elements of the first meshing, the isometric images are given in the figures below.

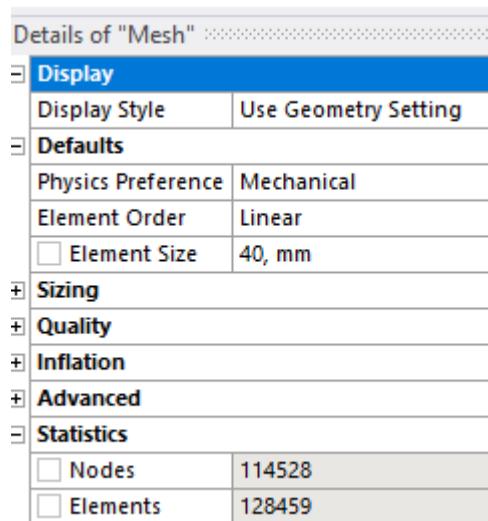


Figure 3.69 First meshing details of the first feeder

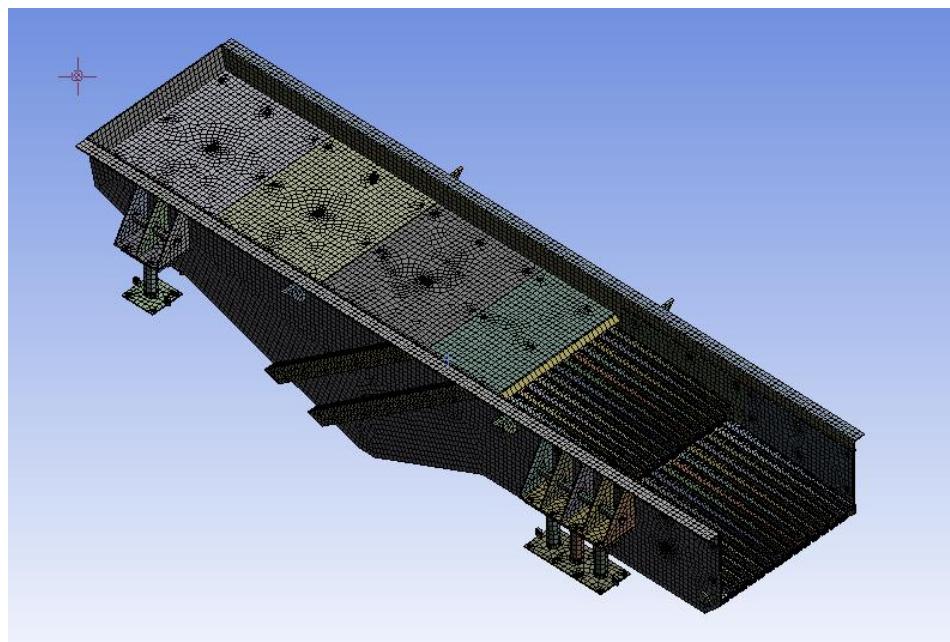


Figure 3.70 First feeder's isometric view after first meshing

Details of "Mesh"	
Display	Display Style <input checked="" type="checkbox"/> Use Geometry Setting
Defaults	
Physics Preference	Mechanical
Element Order	Linear
<input type="checkbox"/> Element Size	40, mm
Sizing	
Quality	
Inflation	
Advanced	
Statistics	
<input type="checkbox"/> Nodes	134975
<input type="checkbox"/> Elements	124351

Figure 3.71 First meshing details of the second feeder

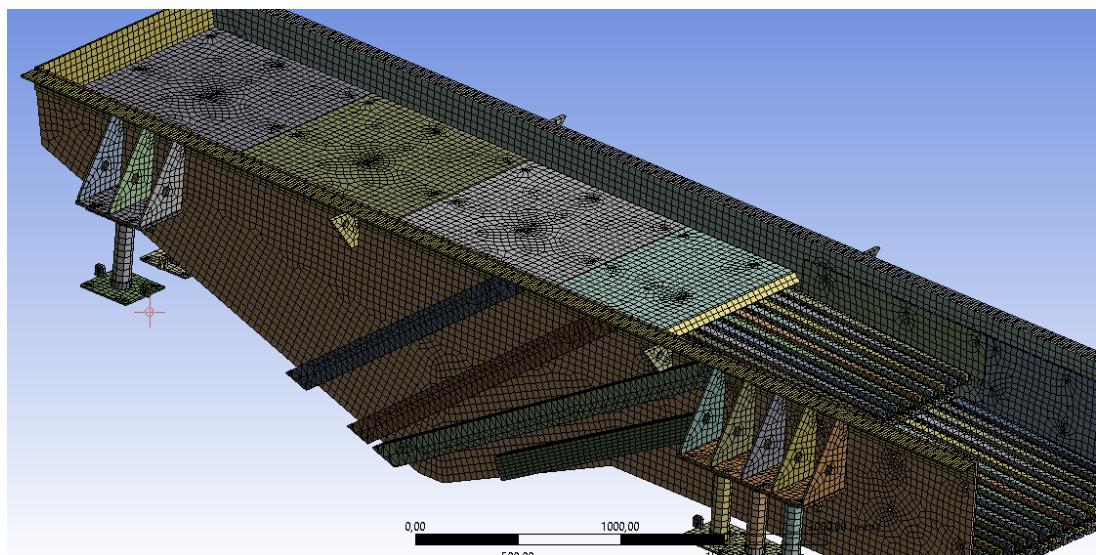


Figure 3.72 Second feeder's isometric view after first meshing

As mentioned above, more detailed analyses were made when the number of nodes and elements in meshing increased. In the thesis, the analysis results as a result of the second meshing (meshing with more nodes and elements numbers) are given. This is because it gives closer and more accurate results to the truth.

The following tables compare the analysis results after the first and second meshing.

Stress Results

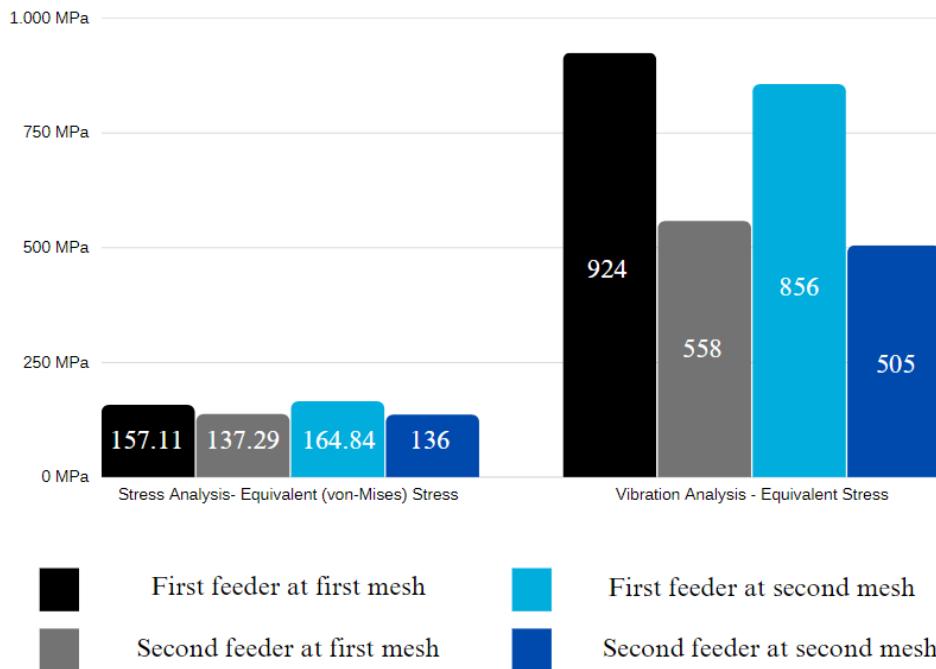


Table 3.2 Stress results from first and second meshings for first and second feeders

Total Deformation Results

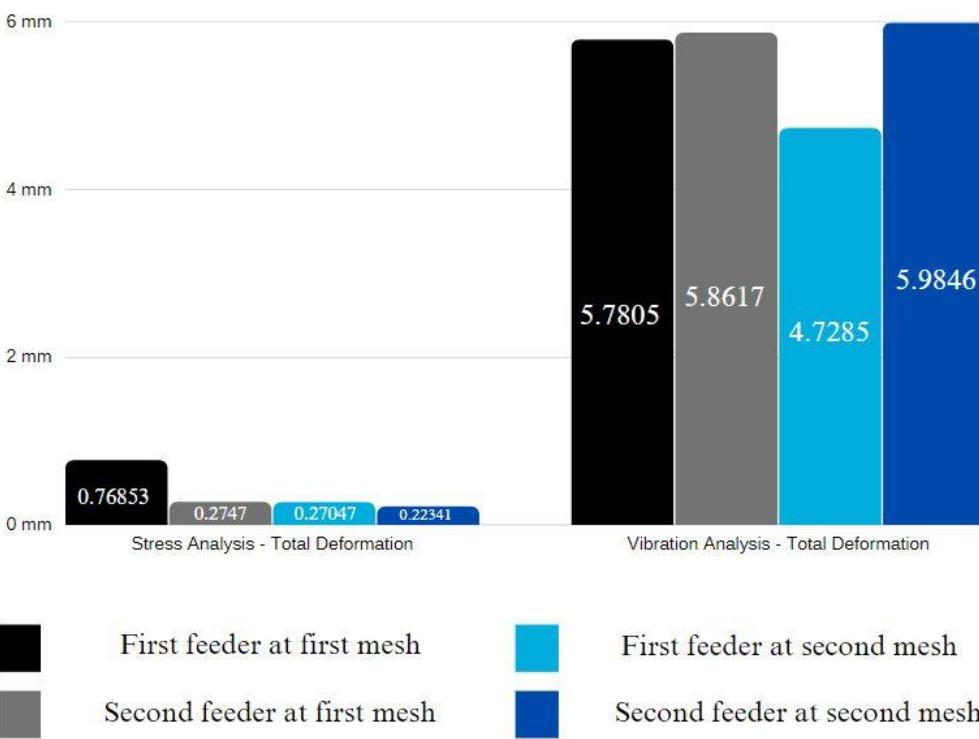


Table 3.3 Total deformation results from first and second meshings for first and second feeders

Fatigue Analysis Results

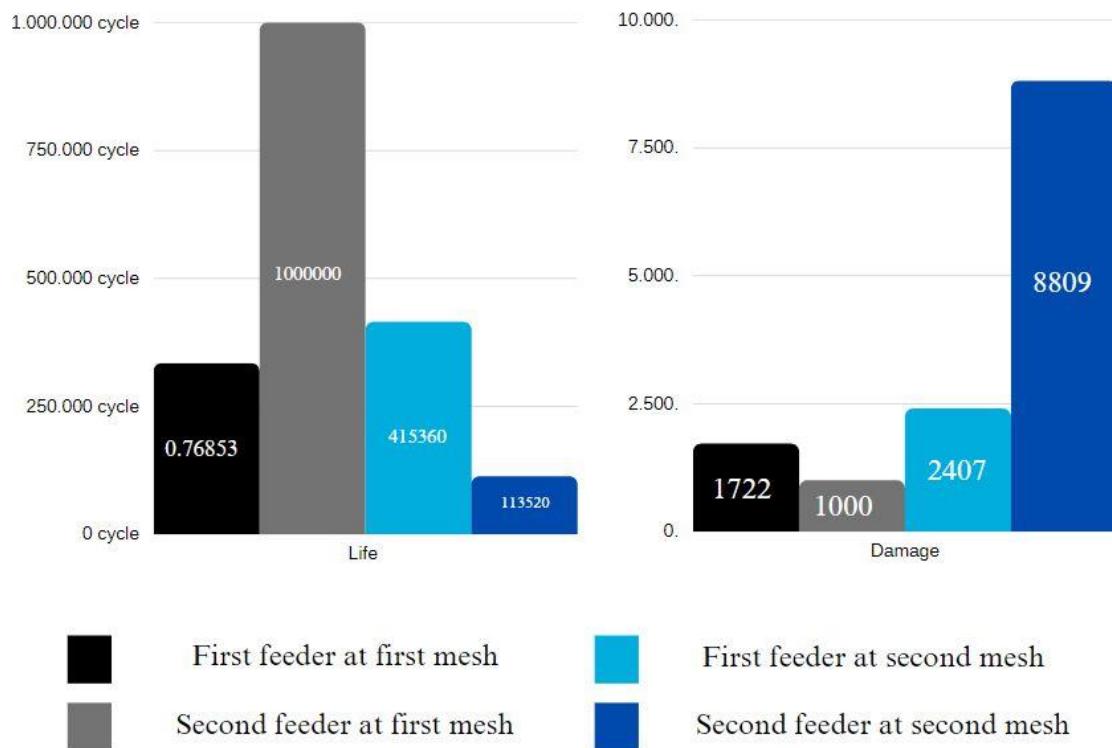


Table 3.4 Fatigue analysis results from first and second meshings for first and second feeders.

4. CONCLUSION AND DISCUSSION

4.1 Conclusion of Thesis

It was the objective of the BURCELIK's investigation to examine two distinct designs of feeders. As reported by the manufacturer, the initial feeder, after a period of use, experienced breakage of its side plates, rendering it inoperable. Consequently, a second feeder design was developed, with the primary distinguishing feature being the supports in their side views. The second feeder operated flawlessly.

To conduct the required static and dynamic analyses, three significant assessments were conducted: stress analysis, fatigue analysis, and vibration analysis. These analyses needed to be highly accurate and free of errors to ensure their applicability and real-life usability. Several preparatory steps were meticulously carried out to facilitate precise and error-free analyses, which were conducted using the available data, information, and documentation.

The stress analysis yielded three distinct analytical findings: total deformation, equivalent elastic strain, and equivalent (von-Mises) stress. In terms of total deformation, upon examining both feeders, the first feeder (previously manufactured) exhibited the maximum deformation of 0.76583 mm, while the least distortion observed was 0, indicating the absence of deformation spots or areas. The central section and side plates of the feeder experienced the greatest impact from the applied loads, as depicted in the Figure accompanying the stress analysis results of the first feeder.

The springs displayed minimal distortion, with only the arc nearest to the center exhibiting some deformation due to the influence of the center of gravity. Notably, a circular region of yellow distortion was observed amidst the green markings in the area where the center of gravity is situated. This distortion resulted from the connection between the mines and the grid. Plus, it should be noted that the red deformation value was only present on the right side of the machine when viewed from the front, suggesting a possible error.

Regarding the stress analysis of the second feeder, it was determined that the side supports effectively functioned, leading to a more uniform distribution of deformation. The maximum deformation value, indicated by the red color, was measured as 0.67447 mm,

which was lower than that of the first feeder, suggesting the effectiveness of the updates implemented in the second feeder.

When comparing the equivalent elastic strain of the two feeders, it was observed that the first feeder displayed the highest value of 0.00087838 (indicated by red), primarily attributed to the elasticity of the springs. Plus, a small degree of comparable elastic strain was observed on the side walls of the first feeder. Contrary to, the grids and top plates exhibited the lowest values, represented by a dark blue hue. The comparable elastic strain value for the first feeder was determined to be 0.000013046 (dark blue). Similar observations were made for the second feeder, with a maximum equivalent elastic strain of 0.00085348 and a minimum value of 0.000012006. Notably, comparable elastic strain was not recorded on the side walls of the second feeder, which can be attributed to the support added during the upgrade, effectively reducing the corresponding strain in the side plates.

The stress analysis concluded with the examination of the equivalent (von-Mises) stress. The first feeder exhibited a maximum stress reading of 157.11 MPa, while the lowest recorded value was 0.00013024 MPa. For the second feeder, these values were 137.2903 MPa (maximum) and 0.00011149 MPa (minimum). Evaluating the equivalent stress analysis of the first feeder revealed significantly larger red spots and areas compared to those of the second feeder. The inclusion of supports on the side plates during the upgrade effectively reduced the equivalent stress in the second feeder.

Following the stress analysis, the vibration analysis was initiated, encompassing three analytical findings similar to the stress analysis: equivalent stress, total deformation, and elastic strain.

During the analysis of equivalent stress in the first feeder, it was determined that the highest equivalent stress with vibration reached 924.31 MPa, while the lowest stress recorded was 0.0009265 MPa. The average equivalent stress was calculated to be 24,036 MPa. Contrary to, the second feeder exhibited a maximum stress measurement of 558.02 MPa, with the lowest stress value at 0.00037653 MPa. The average stress value for the second feeder was determined to be 26,224 MPa. Comparing the two feeders in this regard reveals a significant difference, with a maximum stress difference of 366.29 MPa.

This disparity holds considerable importance as it signifies the success of the upgrade and development efforts undertaken for the second feeder. But while the highest stress level experienced a substantial decrease, the average stress level appears to have risen. Notably, the activation of the vibration motors caused an increase in tension.

During the vibration analysis, it was observed that the first feeder exhibited the greatest deformation during vibration, measuring 5.7805 mm. Conversely, the second feeder had a maximum deformation value of 5.8617 mm. Despite the presence of vibration in both feeders, certain regions and areas showed no deformation, as indicated in the pre-vibration stress study.

Concluding the vibration analysis, the values of Normal Elastic Strain were obtained.

4.2 Recommendations for Future Works

Computerized analysis may only sometimes be correct. Some extras can be done to get more accurate and realistic results for future studies on this subject.

While working on this project, the vibration data in the available data were made by looking at a single report. For future works, vibration data can be tested more extensively, and more accurate results can be obtainable.

Performing and comparing ANSYS analyzes feeder with a real feeder in a real environment will give more accurate results.

Structural Steel assigned in the drawings sent by the company was used as the material instead of plate spring etc, instead of plate spring etc. More accurate results can be obtained using the materials in which all parts are used and these material properties in the engineering data section.

More accurate results can be obtained if the FRP test is performed on the real feeder and the results can be compared.

Performing modal testing on the real feeder and obtaining, examining, and comparing these results may give more accurate results.

4.3 Evaluation of Current Work from MUDEK Perspective

4.3.1 Economic Analysis

The subject of this graduation project was deemed worthy of a scholarship by TUBITAK 2209-B, and financial support was provided to us, the students of this project. We used this support under the name of system development. We could perform our analyses faster with improvements such as RAM and SSD. In this way, we have saved time. Again, with these system improvements, we could perform detailed analyses that our computers were incapable of in the past.

4.3.2 Real-Life Conditions

Our analyzes can be used in real life. It's close to the truth. This is because when we compare the first feeder with the second feeder, we get the output that the problems are reduced, and the operation will be carried out without any problems. Of course, the computer environment analyses may give different results than in real life because some factors cannot be defined in a computer environment. Therefore, it is recommended to give more minimum values.

4.3.3 Productivity

As mentioned in the Recommendations for Future Works section, if the feeder tests are carried out correctly and entirely in the real environment and compared with the analysis in the computer environment, the accuracy of the analyses made on the computer can be proven. When the accuracy of computer analysis is proven, we can make the obtained outputs usable in production.

4.3.4 Constraints

The limitations of our computers caused us to work with a few elements and nodes during the Mesh process. By using a better computer, more accurate and more detailed analysis results can be obtained. We must catch up in time as we have done these analyses by learning the ANSYS program from scratch. Such analyses will be faster and easier if done by someone who knows at least a little about ANSYS. More factors can be examined in depth.

REFERENCES

1. Al-Khzali H, Askari M (2011), Condition monitoring and fault diagnosis in rotating machinery using modal test and finite element analysis. In: Proceedings of the 4th International conference on computational mechanics and virtual engineering, pp. 269–277
2. Carr, A. J. (1994). Dynamic analysis of structures. *Bulletin of the New Zealand Society for Earthquake Engineering*, 27(2), 129-146.
3. Chandravanshi, M. L., & Mukhopadhyay, A. K. (2015). Experimental modal analysis of the vibratory feeder and its structural elements. *International Journal of Applied Engineering Research*, 10 (13), 33303-33310.
4. Chandravanshi, M. L., & Mukhopadhyay, A. K. (2017). Analysis of variations in vibration behavior of vibratory feeder due to change in stiffness of helical springs using FEM and EMA methods. *Journal of the Brazilian Society of Mechanical Sciences and Engineering*, 39, 3343-3362.
5. Chao Paul C P, Shen Chien-Yu (2007) Dynamic modeling and experimental verification of a piezoelectric part feeder in a structure with parallel bimorph beams. *Ultrasonic* 46:205–218
6. Childs, T. H. C. (2021). *Mechanical Design: Theory and Applications*. Butterworth-Heinemann.
7. Coffin, L. F. (1979). Fatigue in Machines and Structures. In Fatigue and Microstructure. American Society for Metals.
8. Csizmadia, B., Hegedűs, A., & Keppler, I. (2011). Optimization of a vibrating Screen's mechanical parameters. In *IUTAM Symposium on Dynamics Modeling and Interaction Control in Virtual and Real Environments: Proceedings of the IUTAM Symposium on Dynamics Modeling and Interaction Control in Virtual and Real Environments, Held in Budapest, Hungary, June 7–11, 2010* (pp. 145-152). Springer Netherlands.
9. Ewins DJ (2000) Basics and state-of-the-art of modal testing. *Sadhana* 25(3):207–220

10. Gao Xueqin, Han Xiaoming,in:The dynamic response of the finite element analysis on Circle vibrating screen box, *Coal Mine Machinery*, 2008,29(11):63~165.
11. Kelly AD, Knight CE (1992), Dynamic finite element modeling and analysis of a hermetic reciprocating compressor. In: *Proceedings of international compressor engineering conference*, Paper no. 869
12. McMillan Jr, G. J. (2011). Analysis of Vibratory Equipment Using the Finite Element Method (Doctoral dissertation, University of Wisconsin--Stout).
13. Pinjarla P, Lakshmana KT (2012) Design and analysis of a shock absorber. *Int J Res Eng Technol* 1(4):578–592
14. Pope, J. E. (1997). Fatigue. In Rules of Thumb for Mechanical Engineers: A Manual of Quick, Accurate Solutions to Everyday Mechanical Engineering Problems (pp. 320-351).
15. Ramatsetse, B. I., Matsebe, O., Mpofu, K., & Desai, D. A. (2013). Conceptual design framework for developing a reconfigurable vibrating screen for small and medium mining enterprises. *SAIE25 Proceedings, Stellenbosch, South Africa*, 1.
16. Ramsey, K. (1983). Experimental modal analysis, structural modifications and FEM analysis on a desktop computer. *Sound and Vibrat.* 17(2), 19-27.
17. Raoa, P. S. (2012). Experimental and analytical modal analysis of welded structure used for vibration based damage identification. *Global Journals of Research in Engineering*, 12(A1), 45-50.
18. Samrudhi, R. S., Dhande, K. K., Singh, V., & Jamdar, N. I. (2014). Modal and harmonic analysis in a stepped vibratory bowl feeder. *Int. Eng. Res. Technol*, 3, 121-130.
19. Wang, B. T., & Cheng, D. K. (2008). Modal analysis of mdof system by using free vibration response data only. *Journal of Sound and Vibration*, 311(3-5), 737-755.
20. Wang, Y. Y., Shi, J. B., Zhang, F. F., Lu, H. L., & Xu, F. (2012). Optimization of vibrating parameters for large linear vibrating screen. In *Advanced Materials Research* (Vol. 490, pp. 2804-2808). Trans Tech Publications Ltd.
21. Li, Y. F., Li, Y. Z., Pan, D. M., Zhang, X. C., & Bao, Y. X. (2008). Determination parameters of kinematics for rectilinear vibrating screen. *Coal Mine Machinery*, 29(3), 33-34.

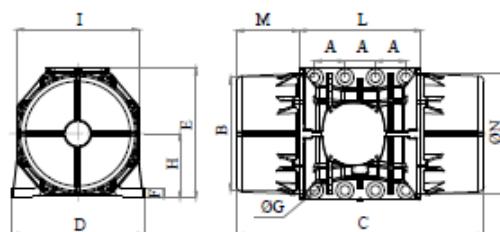
22. Yue-min, Z., Chu-sheng, L., Xiao-Mei, H., Cheng-Yong, Z., Yi-bin, W., & Zi-ting, R. (2009). Dynamic design theory and application of large vibrating screen. *Procedia Earth and Planetary Science*, 1(1), 776-784.
23. Zhang Yongfeng, Z., Zhongjun, Y., Ming, X., (2005), in:Dynamic stress analysis of Vibrating screen, *Metallurgical Equipment*, 4(2):42-43.

APPENDICES



MVE 19500/1E-105A0 (EE619500A5A08A0000)
3 PH - 6 kutup - 1000 d/d - 380-415 V [Delta] - 50 Hz

Çalışma momenti (Kg*cm)	Vibratör çekicileri (Kg*cm)	Santrifüj kuvveti (Kg)	Nominal voltaj (V)	Giriş gücü (kW)	Akım (A)	Güç faktörü	Ia/In
3.632	1.816	20.285	380-415 [Delta]	11,96	△ 24	0,72	5,4



*Technical drawings are illustrative purposes only, please refer to 3D/2D drawings available on "FINDER" app.
Contact us for more information.

TÜM EBATLAR (mm)													
Ağırlık (Kg)	A	B	G	Delik sayısı	C	D	E	F	H	I	L	M	N
768	140	480	45	8	1.060	570	542	48	268	510	560	250	490

TEKNİK ÖZELLİKLER						
Gres tipi	Yaglamasız	Vida	Pul	Sıkma torku (Nm)	Kablo tipi	Kablo rakoru
Please refer to the label on the motorvibrator	Evet	M42	43 x 78 mm	2850	4G6 110°C	M32 110°C

RULMAN ÖMÜR SAATLERİ				
Rulman modeli	Tip	100% Vurma Kuvveti	80% Vurma Kuvveti	50% Vurma Kuvveti
NJ2322	■	6652	13996	67051

SERTİFİKASYON						
ATEX II2 D Ex tb IIIC Tx Db IP66						
IECEx Ex tb IIIC Tx Db IP66						
CLASS II DIV.2 GROUP F,G T4						
Ex tb IIIC Tx Db IP66						
[Tx Size Micro,10-30-100°C - Tx Size 40-91-135°C]						
CONF TO UL1004-3, UL1004-1,UL 60079-0,UL60079-31						
CERT. CSA C22.2 No.100,CSA C22.2 No.77, CSA C22.2N.60079-0,CSA C22.2N.60079-31						
T.Amb.-20/+40°C						

REV1-22/05/2019

Dimension with coarse degree of accuracy related to UNI 22768/1 Rights reserved to modify technical specifications.



ASİL ÇELİK
SANAYİ ve TİCARET A.Ş.
www.asilcelik.com.tr

KALİTE BELGESİ

QUALITY CERTIFICATE/MILL TEST CERTIFICATE

EN 10204-3.1

Müşteri	AKÇELİK DEMİR ÇELİK SAN.VE TİC A.Ş.	Tarih	24.01.2022
Döküm no	D2210202	Kalite	61 SICR 7
Kesit	Yuvarlak 32,00 mm	Ağırlık	15.120 KG
Müşteri Sipariş no	44846	Adet	250
Sipariş no / Kalem no	1100056966 / 000010	Döküman Norm / No	EN 10204/3.1 - 2201058

Malzeme

SICAK BİÇİMLENDİRİLMİŞTİR.

MALZEMELER TAMAMLMASIZ ÜRETİLMİŞTİR.

Çelik Yapım Metodu:

Ark Ocağı/EAF, Pota Fırını/LF, Vakumda Gaz Alma/VD

Pota Kimyasal Analizi (%)

C	Si	Mn	P	S	Cr	Mo	Ni	Al	Cu	Sn
Min	0,57	1,60	0,70		0,20					
Max	0,65	2,00	1,00	0,025	0,025	0,45				
Ölçülen	0,60	1,77	0,75	0,011	0,006	0,30	0,05	0,10	0,022	0,16

Sertlik

Müşteri Şartı	Asıl Çelik Değeri			Birim	Test Yeri	Standard
	Min	Max	Sertlik			
			331	HB	Yüzey	EN ISO 6506-1

Ultrasonik Testi

"ULTRASONİK HATA GARANTİSİ VERİLMEMEKTEDİR."

Yüzey Çatlak Testi

"YÜZEY ÇATLAK TESTİ GARANTİSİ VERİLMEMEKTEDİR."

"MALZEMELERE RADCOMM RC 4069-2 CİHAZI İLE RADYASYON TESTİ UYGULANMIŞTIR."

"YUKARIDA BELİRTİLEN MALZEMELERİN TEST EDİLDİĞİ VE SİPARİŞ ŞARTLARINA UYGUN OLDUĞU ONAYLANIR."

ONAYLAYAN Mehmet Erdal TÜRKAN

33.23.1655.A4[1]

Santral / Central	İç Satış / Domestic Sales	Diş Satış / Export	Fabrika/Plant:	Vergi Dairesi: Büyükküçük Vergi Dairesi Başkanlığı
Tel.: +90 224 280 61 00	+90 262 781 60 50	+90 262 781 60 30	Gemic Mahallesi Gemic Sekâk No: 183	Vergi No: 0860052518
Faks: +90 224 280 62 00	+90 262 781 60 05	+90 262 781 60 05	16800 Orhangazi, Bursa, TURKEY	Ticaret Sicil No.: 18917

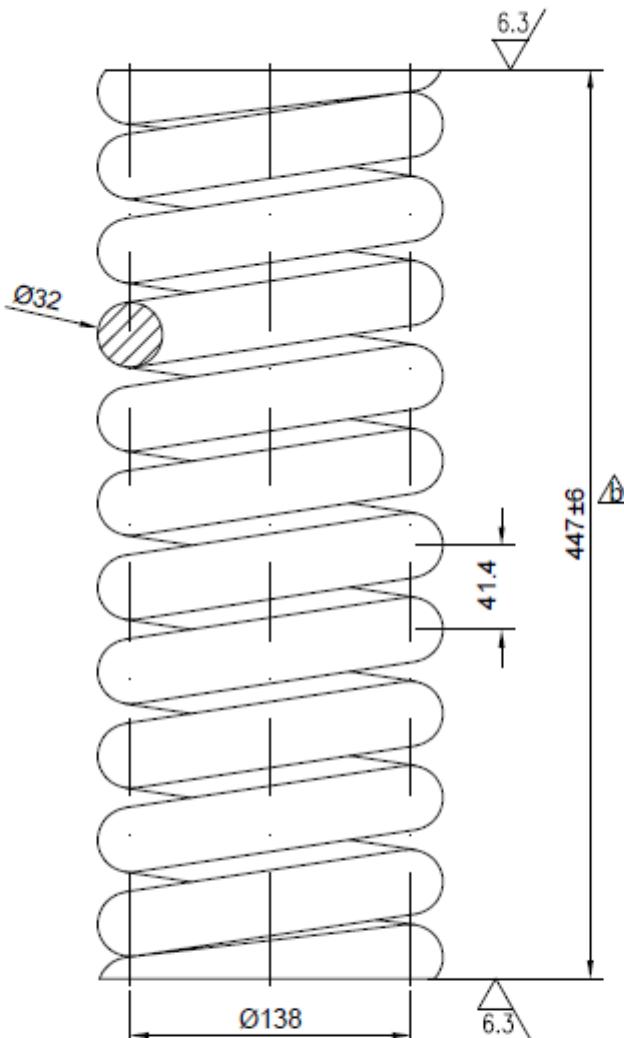


DOSYA NO.

İŞLENMİŞ YÜZEYLER İÇİN TOLERANS VERİLMEMİŞ ÖLÇÜLERDE MÖSAADE EDİLEBİLİR
SAPMALAR [DIN 7168-m]

ÖLÇÜ	0.5-3	3-6	6-30	30-120	120-400	400-1000	1000-2000	2000-4000	4000-8000
MIL	-0.2	-0.2	-0.4	-0.8	-1.0	-1.6	-2.4	-4	-6
DELİK	+0.2	+0.2	+0.4	+0.8	+1.0	+1.6	+2.4	+4	+6
BOY	± 0.1	± 0.1	± 0.2	± 0.3	± 0.5	± 0.8	± 1.2	± 2	± 3

✓ (6.3 ✓)



NOT:
-İki Tarafı taşlanmış kapalı
-Kumlanmış
-if=9,5
-ig=11
C=422 Kg/cm

	05 / 2005	Toleranslar güncellendi.	18.04.2005	N.N.
	REV.	EMİR NO.	DEĞİŞMELER	TARİH İMZA
ÇİZEN	A.KORDE	16.12.2002		
KONTROL	S.ÖMER			
OLÇEK				BURSELİK BURSA ÇELİK DÖKÜM SANAYİ A.Ş.
1/3		YAY	RS.NO.	BT-12-0001-4b
			TİPİ	BT 140x1360
EBADI:	MALZ.: SAE 9262		NET Kg:	Brüt Kg:



ESTETİK YAY SAN. ve TİC. LTD. ŞTİ.



DENEY RAPORU

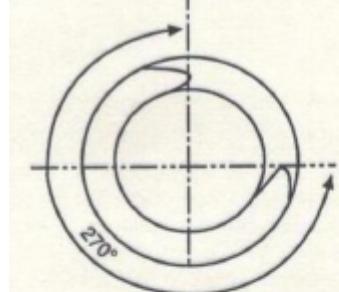
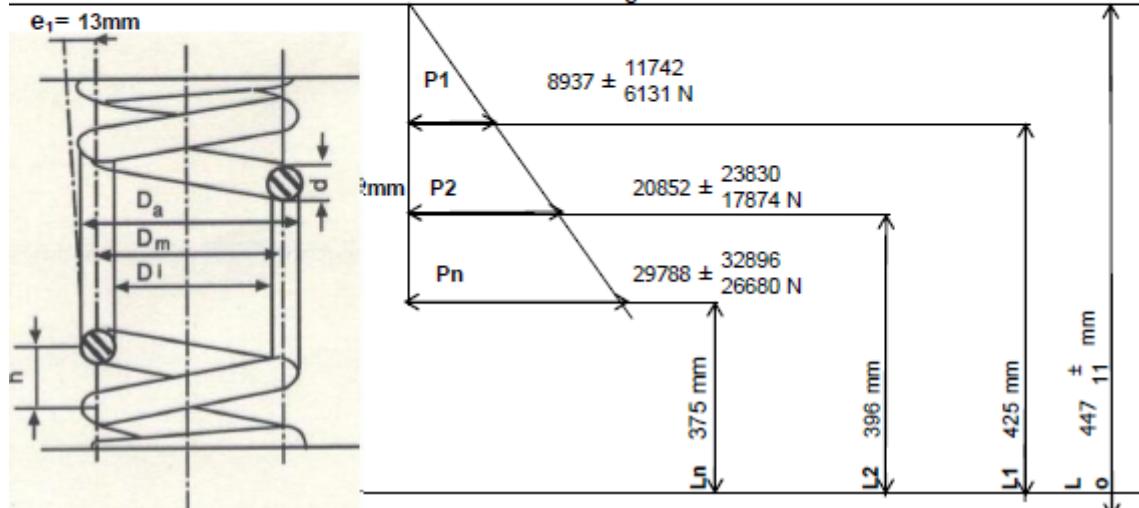
DENEY TARİHİ : 17.02.2023

DENEY STANDARTLARI :

TS 1441-1



Teorik karakteristik eğrisi



Ürün Kodu : ESH-32-003
Sipariş No : 02/0295
Ürünün Tanıtılması : Q32X138X11X447MM
Malzeme Kalitesi : 61SiCr7
Müşteri : BURÇELİK
Resim No :
Sipariş Adedi : 13
Test Adedi : 3
Not : LbL mm'ye kadar basınız

Sıra No	Yayın Çapı d mm	Yay Uz Çapı Da mm	Yay İç Çapı Di mm	Toplam Sarım İğ	Serbest Boy Lo mm	Yüzey Sertliği H.R.C.	Statik Dinamik Yük O N	O kaçıklığı e1 mm	Eksen kaçıklığı e1 mm	Yaylanma Miktarı mm
1	32	171	107	11	449	44	9070	12	24,00	
2	32	171	107	11	451	45	10250	10	26,00	
3	32	171	107	11	451	46	9850	8	26,00	

Boya Kalınlığı : Deney No : T.02.71
 Rapor Tarihi : 17.02.2023
 Adı ve Soyadı : Muhsin AÇIKTEPE
 İmza : Tuna EZİM